THE JOURNAL OF COMPARATIVE NEUROLOGY 459:407–425 (2003)

Loss of Interneurons Innervating Pyramidal Cell Dendrites and Axon Initial Segments in the CA1 Region of the Hippocampus following Pilocarpine-Induced Seizures

CELINE DINOCOURT,[1,3] ZDRAVKO PETANJEK,[1,2] TAMAS F. FREUND,[3] YEZEKIEL BEN-ARI,[1] AND MONIQUE ESCLAPEZ[1]*
[1]INMED, INSERM U29, Parc scientifique de Luminy, B.P. 13 13273 Marseille, France
[2]Croatian Institute for Brain Research, School of Medicine, University of Zagreb, 10000 Zagreb, Croatia
[3]Institute of Experimental Medicine, Hungarian Academy of Sciences, H-1450 Budapest, Hungary

ABSTRACT

In the pilocarpine model of chronic limbic seizures, vulnerability of GABAergic interneurons to excitotoxic damage has been reported in the hippocampal CA1 region. However, little is known about the specific types of interneurons that degenerate in this region. In order to characterize these interneurons, we performed quantitative analyses of the different populations of GABAergic neurons labeled for their peptide or calcium-binding protein content. Our data demonstrate that the decrease in the number of GAD mRNA-containing neurons in the stratum oriens of CA1 in pilocarpine-treated rats involved two subpopulations of GABAergic interneurons: interneurons labeled for somatostatin only (O-LM and bistratified cells) and interneurons labeled for parvalbumin only (basket and axo-axonic cells). Stratum oriens interneurons labeled for somatostatin/calbindin or somatostatin/parvalbumin were preserved. The decrease in number of somatostatin- and parvalbumin-containing neurons was observed as early as 72 hours after the sustained seizures induced by pilocarpine injection. Many degenerating cell bodies in the stratum oriens and degenerating axon terminals in the stratum lacunosum-moleculare were observed at 1 and 2 weeks after injection. In addition, the synaptic coverage of the axon initial segment of CA1 pyramidal cells was significantly decreased in pilocarpine-treated animals. These results indicate that the loss of somatostatin-containing neurons corresponds preferentially to the degeneration of interneurons with an axon projecting to stratum lacunosum-moleculare (O-LM cells) and suggest that the death of these neurons is mainly responsible for the deficit of dendritic inhibition reported in this region. We demonstrate that the loss of parvalbumin-containing neurons corresponds to the death of axo-axonic cells, suggesting that perisomatic inhibition and mechanisms controlling action potential generation are also impaired in this model. J. Comp. Neurol. 459:407–425, 2003.

Indexing terms: temporal lobe epilepsy; rat; GAD; somatostatin; parvalbumin; fluoro-jade B

Vulnerability of subpopulations of GABAergic neurons to seizure-induced damage has been reported in two major regions of the hippocampal formation in experimental and human temporal lobe epilepsy (TLE). The loss of GABAergic interneurons is now well demonstrated in the hilus of the dentate gyrus in several models of TLE (Obenaus et al., 1993; Houser and Esclapez, 1996; Buckmaster and Jongen-Relo, 1999) and the vulnerability of specific subpopulations of hilar interneurons including somatostatin- and parvalbumin-containing neurons is established in experimental (Sloviter, 1987; 1991; Ylinen et al., 1991; Sperk et al., 1992; Magloczky and Freund, 1995; Buckmaster and Dudek, 1997; Gorter et al., 2001) as in

Grant sponsor: Institut National de la Santé et de la Recherche Médicale; Grant sponsor: the Howard Hughes Medical Institute (T.F.F); Grant sponsor: National Institute of Health; Grant number: NS 30549; Grant sponsor: Országos Tudományos Kutatási Alapprogramok Hungary; Grant number: T 32251.

*Correspondence to: Monique Esclapez, INMED, INSERM U29, Parc scientifique de Luminy, 163 Route de Luminy, B.P 13 13273 Marseille, Cedex 9, France. E-mail: esclapez@inmed.univ-mrs.fr

Received 25 July 2002; Revised 13 December 2002; Accepted 20 December 2002

DOI 10.1002/cne.10622

Published online the week of March 24, 2003 in Wiley InterScience (www.interscience.wiley.com).

human TLE (de Lanerolle et al., 1989; Robbins et al., 1991; Mathern et al., 1995; Magloczky et al., 2000; Wittner et al., 2001).

More recently, the vulnerability of GABAergic interneurons in the stratum oriens of CA1 has been demonstrated in several models of TLE (Houser and Esclapez, 1996; Morin et al., 1998; Andre et al., 2001; Cossart et al., 2001) and, as in the hilus of the dentate gyrus, these neurons included some somatostatin- and parvalbumin-containing neurons (Best et al., 1993,1994; Cossart et al., 2001; Bouilleret et al., 2000; Andre et al., 2001). However, little is known about the specific morphological types of interneurons associated with these degenerating subpopulations of GABAergic neurons identified on the basis of their neurochemical content.

Such characterization is important, since these different subtypes of interneurons may have different functional properties and their loss may lead to different functional consequences.

In CA1, somatostatin-containing neurons with their somata mainly located in stratum oriens have been thought to belong exclusively to the class of dendritic inhibitory cells (i.e., interneurons innervating pyramidal cell dendrites; for review, see Freund and Buzsáki, 1996), in particular to those with an axon projecting to stratum lacunosum-moleculare (O-LM cells), or to both strata radiatum and oriens (bistratified cells) (Sik et al., 1995; Maccaferri et al., 2000). However, some interneurons that project to the medial septum and previously described as interneurons coexpressing somatostatin and calbindin (Freund and Buzsaki, 1996; Toth and Freund, 1992) possess many axon collaterals in CA1 that selectively innervate other interneurons (Gulyas et al., 2001). Thus, these cells could be considered as belonging to the class of interneuron-selective interneurons, similar to those that contain calretinin (Gulyas et al., 1996).

Parvalbumin-containing interneurons have been considered for many years to be interneurons exclusively responsible for perisomatic inhibition; they include basket and axo-axonic cells, with an axon innervating the soma and the axon initial segment of pyramidal cells, respectively (Katsumaru et al., 1988). However, in the stratum oriens of CA1 some parvalbumin-containing interneurons also express somatostatin (Bering et al., 1995; Jinno and Kosaka, 2000); these may include O-LM and bistratified cells (Maccaferri et al., 2000; McBain and Fisahn, 2001). Thus, in CA1 some parvalbumin-containing neurons could belong to a class of interneurons that exert dendritic inhibition.

Recent studies demonstrate, in several models of TLE, including the pilocarpine model, a clear deficit of GABAergic inhibitory drive impinging on the dendrites of CA1 pyramidal cells (Cossart et al., 2001), whereas GABAergic inhibition recorded in the soma of these cells remains functional (Esclapez et al., 1997; Rempe et al., 1997; Hirsch et al., 1999; Cossart et al., 2001). Furthermore, GABAergic neurons in the CA1 pyramidal cell layer (Houser and Esclapez, 1996; Esclapez et al., 1999) and the density of GABAergic terminals around the somata of these neurons (Hirsch et al., 1999) are preserved. All these results suggest that interneurons innervating pyramidal cell dendrites (dendritic inhibitory cells) represent the only subpopulation of GABAergic interneurons that undergo damage in CA1.

In order to clarify the issue of selective vulnerability of interneurons responsible for dendritic or perisomatic inhibition in experimental TLE, the aims of this study were: 1) to identify the different subpopulations of GABAergic interneurons in the CA1 region that are sensitive to pilocarpine-induced chronic limbic seizures; and 2) to determine the extent and temporal profile of neuronal loss following pilocarpine-induced status epilepticus. For this purpose, in situ hybridization and immunohistochemical methods were used to identify the entire population of GABAergic neurons in the CA1 subfield and its various subpopulations, including somatostatin-, parvalbumin-, and calbindin-containing neurons in control and pilocarpine-treated animals processed at several intervals after the severe seizure episode induced by the drug. Stereological techniques were used to quantify the distribution and loss of different populations of interneurons in the CA1 region. Electron microscopy and neuronal degeneration methods were used in parallel to confirm the patterns of neuronal death.

Preliminary reports of these findings have been published previously (Dinocourt et al., 2001).

MATERIALS AND METHODS

Animals

Adult male Wistar rats (200–290 g; Charles River, France) were treated with pilocarpine, a muscarinic cholinergic agonist, according to an established procedure (Turski et al., 1983; Cavalheiro et al., 1987; Obenaus et al., 1993). Pilocarpine hydrochloride (325–350 mg/kg, Sigma, St. Louis, MO) was injected intraperitonealy (i.p.) 30 minutes after administration of a low dose of the cholinergic antagonist methyl scopolamine nitrate (1 mg/kg, i.p., Sigma) to minimize peripheral cholinergic effects (Turski et al., 1983). Following pilocarpine injection, 75% of the rats (n = 24) survived the acute seizure period induced by the drug. Only animals that experienced at least 3 hours of sustained complex motor seizures were included in this study (n = 19). To minimize mortality in these animals, the period of severe sustained seizures was stopped by a single injection of valium (6 mg/kg, i.p., Sigma). The rats were then observed 3–4 hours a day in the vivarium for general behavior and occurrence of spontaneous seizures.

Of the animals that developed spontaneous recurrent limbic seizures (n = 10), seven rats were sacrificed 3 months after pilocarpine injection for a detailed quantitative neuroanatomical study of the different subpopulations of GABAergic interneurons in the CA1 region of the hippocampal formation, and three rats were sacrificed for a quantitative electron microscopic study of the synaptic coverage of the axon initial segment of CA1 pyramidal cells. Only seizures of grade 3 or greater on the Racine (1972) scale were scored (i.e., forelimb clonus ± rearing ± falling). The onset of spontaneous seizure occurrence was 4–6 weeks after drug injection.

Other pilocarpine-treated animals that initially showed sustained motor seizures were studied at shorter postinjection intervals (72 hours and 1 and 2 weeks, n = 3 at each interval) to evaluate the time course of neuronal degeneration in the hippocampal formation. These animals displayed normal motor activity, eating and drinking behavior, and no spontaneous seizures during their sur-

vival period. Eight age-matched rats from the same litters were used for control experiments.

All animal use protocols conformed to NIH guidelines and the French Public Health Service Policy on the use of laboratory animals.

Tissue preparation for light microscopy

Rats were deeply anesthetized with sodium pentobarbital injection (60 mg/kg, i.p.) and perfused intracardially with a fixative solution containing 4% paraformaldehyde in 0.12 M sodium phosphate buffer (PB), pH 7.4. Rats received ~300 ml of this fixative per 100 g of body weight. After perfusion the brains were removed from the skull, postfixed in the same fixative for 1 hour at room temperature (RT), and rinsed in 0.12 M PB for 1.5 hours. Blocks of forebrain containing the entire hippocampal formation were cryoprotected in a solution of 20% sucrose in PB overnight at 4°C, quickly frozen on dry ice, and sectioned coronally at 40 μm on a cryostat. Sections were rinsed in 0.01 M phosphate-buffered saline (PBS), pH 7.4, collected sequentially in tubes containing an ethylene glycol-based cryoprotective solution (Watson et al., 1986; Lu and Haber, 1992), and stored at –20°C until histological processing. Before use, PBS and cryoprotective solutions were treated with 0.05% diethylpyrocarbonate and autoclaved to inactive RNase activity.

Every tenth section was stained with cresyl violet in order to determine the general histological characteristics of the tissue within the rostral–caudal extent of the hippocampal formation. From each rat, adjacent sections were processed for: 1) in situ hybridization histochemistry with nonradioactive-labeled riboprobes to detect GAD65 mRNA; 2) single-labeling immunohistochemistry for the detection of GAD67 and parvalbumin; and 3) double-labeling immunohistochemistry for the simultaneous detection of somatostatin/neuronal-specific nuclear protein (NeuN), somatostatin/parvalbumin, and somatostatin/calbindin. In order to perform quantitative stereological analysis of the different populations of interneurons in control and pilocarpine-treated animals, eight sections from each rat, selected at regular intervals within the rostrocaudal extent of the entire hippocampal formation, were processed for each in situ hybridization or immunohistochemical labeling (see below). Other series of sections at similar levels were processed with neuronal degeneration methods (Gallyas and fluoro-jade B). Sections from control and pilocarpine-treated rats were always processed in parallel.

Immunohistochemistry

Antibodies. The rabbit polyclonal antiserum K2, described by Kaufman et al. (1991), was used to label cell bodies and axon terminals of GABA neurons. This antiserum was generated in rabbit after injection of GAD67 that was produced in a bacterial expression system from a cloned feline GAD cDNA (Kaufman et al., 1991; Kobayashi et al., 1987) and purified by sodium dodecyl sulfate polyacrylamide gel electrophoresis (Kaufman et al., 1991). This antiserum recognizes only two proteins, primarily rat GAD67 and, to a lesser extent, GAD65 on Western blots (Kaufman et al., 1991; Esclapez et al., 1994) and tissue sections (Esclapez et al., 1994). Somatostatin-containing neurons were localized with a polyclonal antiserum raised in rabbit (IHC 8001, Peninsula Laboratories, Belmont, CA). The biological and immunohistochemical specificity of the antiserum has been characterized previously. This antiserum recognizes specifically both somatostatin-14 and somatostatin-28, the biologically active peptides (Richoux et al., 1981; Benoit et al., 1985). Parvalbumin was labeled with a monoclonal antibody raised in mice (Swant, Bellinzona, Switzerland; Celio et al., 1988). A mouse monoclonal antibody that recognizes the neuronal-specific nuclear protein (NeuN) (MAB 377, Chemicon International, Temecula, CA) (Mullen et al., 1992) was used to visualize all hippocampal neurons. The mouse monoclonal antibody D-28K (McAB 300, Swant) was used to label calbindin-containing neurons (Celio et al., 1990).

Immunohistochemical methods. All free-floating sections to be processed for immunohistochemistry (IHC) were first rinsed for 30 minutes in 0.02 M potassium PBS (KPBS; 16 mM K_2HPO_4, 3.5 mM KH_2PO_4, 150 mM NaCl, pH 7.4), incubated in 1% hydrogen peroxide for 30 minutes to block endogenous peroxidases, and rinsed in KPBS.

Single immunohistochemical labeling for GAD67 and parvalbumin. This was performed with unlabeled primary antibodies and standard avidin—biotin–peroxidase complex (ABC) methods (Vectastain Elite ABC, Vector Laboratories, Burlingame, CA). Sections processed for GAD67-IHC were incubated for 1 hour at room temperature (RT) in KPBS containing 3% normal goat serum (Vector Laboratories) and overnight at RT in K2 antiserum diluted 1:4,000 in KPBS containing 1% normal goat serum. Sections processed for parvalbumin-IHC were incubated for 1 hour at RT in KPBS containing 0.3% Triton X-100 (KPBS–Triton) and 3% normal horse serum (Vector Laboratories), and overnight at RT in parvalbumin monoclonal antibody diluted 1:4,000 in KPBS-Triton containing 1% normal horse serum. After these steps, sections were rinsed for 30 minutes in KPBS and incubated for 1 hour at RT in biotinylated goat antirabbit immunoglobulin G (IgG) or horse antimouse IgG (Vector Laboratories) diluted 1:200 in KPBS containing 3% normal goat serum or normal horse serum. Sections were then rinsed in KPBS, incubated for 1 hour at RT with an ABC solution prepared according to the manufacturer's recommendations (Vector Laboratories). After several rinses in KPBS, sections from control and pilocarpine-treated animals were processed for the same time (10 minutes) in 0.04% 3-3′-diaminobenzidine-HCl (DAB) and 0.006% hydrogen peroxide diluted in KPBS. The sections were then rinsed in KPBS, mounted on gelatin-coated slides, dried, dehydrated, and coverslipped with permount (Fisher Scientific, Electron Microscopy Sciences, Washington, PA).

Immunohistochemical controls for single labeling experiments included incubations in rabbit or mouse normal IgG and omission of primary antiserum or antibody. No labeling of neuronal cell bodies, processes, or terminals was observed in these control tissues.

Double immunohistochemical labeling for somatostatin/NeuN, somatostatin/parvalbumin, and somatostatin/calbindin. Sections were incubated for 1 hour at RT in KPBS–Triton containing 2% milk protein (blocking reagent; Roche Molecular Biochemicals, Meylan, France). Sections processed for somatostatin/NeuN-IHC, somatostatin/parvalbumin-IHC, or somatostatin/calbindin-IHC were incubated for 48 hours at 4°C in a mixture of somatostatin antiserum (1:4,000) and NeuN antibody (1:4,000), parvalbumin monoclonal antibody (1:8,000), or calbindin monoclonal antibody (1:8,000) diluted in KPBS–Triton.

For the double immunohistochemical labeling of somatostatin/NeuN, the detection of somatostatin was performed first with standard ABC methods. Sections were incubated for 1 hour at RT in biotinylated goat antirabbit IgG (1:200) diluted in KPBS containing 0.5% milk protein, rinsed in KPBS for 30 minutes, and incubated for 1 hour at RT with an ABC solution prepared in KPBS according to the manufacturer's recommendations. The peroxidase activity was then revealed with 0.04% DAB, 0.03% nickel ammonium sulfate and 0.006% hydrogen peroxide diluted in KPBS (DAB–Nickel) that gave an intense blue reaction product. After this step, sections were extensively rinsed in KPBS and processed for the detection of NeuN antibody with avidin—biotin–alkaline phosphatase (ABC-AP) methods. Sections were incubated for 1 hour at RT in biotinylated horse antimouse IgG (1:200) diluted in KPBS containing 0.5% milk protein, rinsed in KPBS for 30 minutes, incubated for 1 hour with an ABC-AP solution prepared in KPBS according to manufacturer's recommendations. The alkaline phosphatase activity was detected with fast red chromogen (Roche Molecular Biochemicals) diluted 0.1% in 0.1 M Tris HCl, pH 8.2; this resulted in the formation of a red precipitate.

For the double immunohistochemical labeling of somatostatin/parvalbumin or somatostatin/calbindin, sections were incubated for 1 hour at RT in a mixture of biotinylated goat antirabbit IgG (1:200) and Fluorescein horse antimouse (1:100) (Vector Laboratories) diluted in KPBS containing 0.5% milk protein. Sections were then rinsed and incubated for 1 hour in a solution of KPBS containing an antifluorescein antibody conjugated with alkaline phosphatase (1:1,000) (Roche Molecular Biochemicals) and the ABC complex. The alkaline phosphatase activity was first detected by incubating the sections with a Vector red (Vector Laboratories) or fast red chromogen prepared according to the manufacturer's recommendations, which produced an intense red labeling of calbindin- or parvalbumin-containing neurons. After these steps, sections were rinsed intensively and then processed for detection of the peroxidase activity with DAB–Nickel substrates and gave a dark-blue staining of somatostatin-containing neurons.

All sections were mounted on gelatin-coated slides, dried, and coverslipped in an aqueous mounting medium (Crystal/Mount, Biomeda, Foster City, CA) or after dehydration in an organic mounting medium Permount (Fisher Scientific).

Immunohistochemical controls for double labeling experiments included incubations in both rabbit and mouse normal IgG and omission of both primary antiserum and antibody. No specific staining was detected in these control sections. In addition, some sections were incubated in a mixture of one primary antiserum (or antibody) and mouse normal IgG (or rabbit normal IgG). In all cases, these sections displayed the same pattern of immunolabeling than sections processed for single labeling.

In situ hybridization

Probe synthesis. The GAD probes used in this study were digoxigenin-labeled RNA probes, obtained by in vitro transcription of a previously described rat GAD65 cDNA (Erlander et al., 1991). This cDNA (2.4 kb), containing the entire coding region for rat GAD65, was isolated from a λzapII rat hippocampus library and subcloned into the Bluescript transcription vector (SK polylinker, Stratagene Cloning Systems, La Jolla, CA). GAD65 mRNA detection was selected in the present study because previous studies have demonstrated that GAD65 mRNA is present in all subpopulations of GAD- and GABA-containing neurons in the hippocampal formation of normal rats (Houser and Esclapez, 1994). Probe synthesis was performed with the nonradioactive RNA labeling kit (Roche Molecular Biochemicals) as described previously (Esclapez et al., 1993).

Hybridization and detection. Free-floating sections from control and pilocarpine-treated rats were processed for GAD65 in situ hybridization labeling, as described previously (Esclapez et al., 1993), in order to estimate the total population of GABAergic interneurons. In situ hybridization detection of GAD65 mRNA was associated with an immunohistochemical labeling of the NeuN in order to estimate in the same section the total neuronal population. After standard pretreatment to improve penetration of the reagents, the sections were incubated for 1 hour at RT in a prehybridization solution containing 50% formamide, 750 mM NaCl, 25 mM EDTA, 25 mM piperazine-N,N′-bis (2-ethanesulfonic acid) (PIPES), 0.2% sodium dodecyl sulfate (SDS), 0.02% Ficoll, 0.02% polyvinylpyrrolidone, 0.02% bovine serum albumin, 250 μg/ml poly A and 250 μg/ml salmon sperm DNA. Sections were then incubated for 16 hours at 50°C in the hybridization solution containing 0.2 ng/μl digoxigenin-labeled RNA probe, 100 mM DTT, and 4% dextran sulfate. After hybridization, sections were rinsed in a 4 × saline sodium citrate solution (SSC; 1 × SSC: 150 mM NaCl, 60 mM Na citrate, pH 7.0) containing 10 mM sodium thiosulfate, and treated with ribonuclease A (0.05 mg/ml in 0.5 M NaCl, 10 mM sodium thiosulfate, 1 mM EDTA, 10 mM Tris–HCl buffer, pH 7.8) for 30 minutes at 37°C. Low- to high-stringency washes were performed with decreasing concentrations of SSC, ending with an incubation in 0.1 × SSC, 10 mM sodium thiosulfate for 30 minutes at 55°C. Sections were then processed for immunodetection of the digoxigenin label by means of a nucleic acid detection kit (Roche Molecular Biochemicals). The sections were rinsed for 10 minutes in 100 mM Tris–HCl buffer, 150 mM NaCl, pH 7.5 (TBS), immersed for 1 hour in the same buffer containing 0.5% blocking reagent and 0.3% Triton X-100, and then incubated overnight at 4°C in two antisera: the alkaline phosphatase-conjugated sheep antiserum to digoxigenin (1:1,000) and the NeuN monoclonal antibody (1:8,000) diluted in TBS containing 0.3% Triton X-100. On the following day the alkaline phosphatase-labeled antibodies to digoxigenin were visualized first by incubating the sections in a chromogen solution containing nitroblue tetrazolium (NBT) and 5-bromo-4-chloro-3-indolyl phosphate (BCIP) reagents resulting in the formation of a dark-blue product.

After this step, sections were extensively rinsed in TBS and processed for the detection of the NeuN antibody with standard ABC-AP methods. Sections were incubated for 1 hour at RT in biotinylated horse antimouse IgG (1:200) diluted in TBS containing 0.5% blocking reagent, rinsed in TBS, and incubated for 1 hour at RT with an ABC-AP solution prepared in TBS according to manufacturer's recommendations. The alkaline phosphatase activity was then revealed with a fast red chromogen diluted in 0.1 M Tris HCl, pH 8.2. Finally, the sections were mounted on gelatin-coated slides, dried, and coverslipped in an aqueous mounting medium (Crystal/Mount, Biomeda).

TABLE 1. Mean Numbers of Counted Neurons and Coefficients of Error

	Stratum oriens		Stratum pyramidale		Stratum radiatum/ lacunosum-moleculare	
Neurons labeled for GAD65 mRNA	Control	Pilo	Control	Pilo	Control	Pilo
N	496 ± 43	235 ± 43	304 ± 12	205 ± 24	548 ± 44	648 ± 21
CE*	0.05	0.06	0.07	0.07	0.05	0.05
Parvalbumin						
N	221 ± 13	96 ± 13	231 ± 18	224 ± 7	28 ± 3	38 ± 3
CE*	0.07	0.092	0.07	0.07	0.1	0.097
Somatostatin-						
N	340 ± 27	200 ± 35	65 ± 11	48 ± 6	18 ± 5	20 ± 3
CE*	0.06	0.09	0.09	0.094	0.11	0.12
Stratum oriens	Neurons only labeled for somatostatin		Neurons only labeled for calbindin		Neurons labeled for somatostatin/calbindin	
	Control	Pilo	Control	Pilo	Control	Pilo
N	412 ± 48	175 ± 16	48 ± 7	54 ± 14	104 ± 15	108 ± 10
CE*	0.05	0.06	0.095	0.095	0.09	0.09
Stratum oriens	Neurons only labeled for Somatostatin		Neurons only labeled for Parvalbumin		Neurons labeled for Somatostatin/Parvalbumin	
	Control	Pilo	Control	Pilo	Control	Pilo
N	360 ± 50	209 ± 51	79 ± 19	52 ± 6	61 ± 18	51 ± 6
CE*	0.06	0.08	0.091	0.095	0.091	0.097

*Coefficient of error (CE) is the mean of the coefficients of error of individual estimates.

Neuronal degeneration methods

Silver impregnation and fluoro-jade B methods were used to identify degenerating neurons in tissue from animals sacrificed at short time intervals after pilocarpine injection.

Silver impregnation method. This was a modification of the methods of Gallyas et al. (1980) described in detail by Nadler and Evenson (1983).

Fluoro-jade B method. This was performed as described by Schmued and Hopkins (2000). Briefly, sections were rinsed in 0.12 M PB, mounted on 2% gelatin-coated slides, and air-dried on a slide warmer at 50°C overnight. Sections were then immersed in a solution containing 1% sodium hydroxide in 80% alcohol for 5 minutes, rehydrated quickly, incubated in 0.06% potassium permanganate for 10 minutes, rinsed in distilled water, and incubated in a solution of 0.0004% fluoro-jade B (Histo-Chem, Jefferson, AR). Sections were then rinsed in distilled water, dried at 50°C for 5–10 minutes, immersed in xylene, and coverslipped with permount (Fisher Scientific). The analysis was performed using a confocal microscope (Olympus fluoview laser scanning microscope, Germany).

Quantitative analysis

Quantitative analysis was performed by two investigators who were blind to the experimental group treatment. The numbers of interneurons labeled for GAD65 mRNA, somatostatin, parvalbumin, calbindin in stratum oriens/alveus, stratum pyramidale, and stratum radiatum/lacunosum-moleculare, and the numbers of interneurons double-labeled for somatostatin/parvalbumin and somatostatin/calbindin in the stratum oriens of the CA1 region in control and pilocarpine-treated animals were estimated by using the optical fractionator method (West et al., 1991; West, 1999). The total number of neurons labeled with NeuN was estimated similarly in stratum oriens/alveus and in stratum radiatum/lacunosum-moleculare. These analyses were performed with a computer-assisted system using the Stereo Investigator software (MicroBrightField, Baltimore, MD). The computer assisted system included a PC connected to a color video camera (DEI-470, Optronics, Santa Barbara, CA) connected to a Nikon microscope (Optiphot, Nikon, Melville, NY). The microscope was equipped with a 3D motorized stage (MAC 2000, Ludl Electronic Products, Hawthorne, NY) and a linear focus encoder providing a 0.25 μm accuracy of absolute focus position (Heidenhein Corp., Schaumburg, IL) allowing accurate stereological analysis with a 20× lens (1900× final magnification). Similar numbers were obtained in a pilot study with 20×, 40×, and 100× objectives; thus, we were confident with using the 20×. Starting from a random position, the number of sections analyzed per hippocampus, for each in situ hybridization or immunohistochemical labeling, was eight. In each section three regions of the CA1 area were delineated: the stratum oriens/alveus, which extended from the pial surface of the ventricula to the outer edge of the pyramidal cell layer; the stratum pyramidale, which included the pyramidal cells; and the stratum radiatum/lacunosum-moleculare, which extended from the edge of the pyramidal cell layer to the hippocampal fissure. The lateral borders of CA1 were delineated by straight lines perpendicular to the pyramidal cell layer at the limit with CA3 and the subiculum. Neurons were counted within a probe volume defined by the counting frame and the dissector height. The dissector height (20 μm) used in this study is the real thickness of sections (24 μm) minus 2 μm on each side of the section to exclude the regions showing irregularities due to cut processes. The real thickness of sections (24 μm) resulted from shrinkage of the sections (40 μm thick) following histological treatment. The size of the counting frame was 100 × 100 μm. Only neurons within the counting frame or overlapping the right or superior border of the counting frame, and which came into focus while focusing down through the dissector height, were counted. To estimate the number of labeled neurons for each region of CA1 (stratum oriens/alveus, stratum pyramidale, stratum radiatum/lacunosum-moleculare) and per hippocampus, each region was entirely sampled (counting frame, 100 × 100 μm; counting grid 100 × 100 μm) randomly and systematically. The average number of neurons counted per region and hippocampus is indicated in Table 1. The precision of each

estimate was controlled by measuring the coefficient of error (CE), which is the mean of the coefficients of error of the individual estimates (West et al., 1991; West, 1999). The CE was 10% or less for each estimated number of labeled neurons (Table 1).

The total numbers of neurons labeled for GAD65 mRNA, somatostatin, parvalbumin, calbindin, and NeuN per region of the CA1 area of each hippocampus were estimated by the software. The average estimated total number of labeled neurons ± SEM was calculated for each group of control and pilocarpine-treated rats. The data were analyzed statistically with a mixed model analysis of variance (ANOVA) and Student's *t*-test to determine significant differences in the number of neurons per area between groups (control and pilocarpine-treated rats) in each region and each interval (3 months, 1 and 2 weeks, 72 hours). The extent of neuron loss in pilocarpine-treated rats was calculated with the following formula: [100 – (100 × average estimated number of neurons in pilocarpine-treated rats ÷ average estimated number of neurons in control rats)]%.

Electron microscopy

Tissue preparation. Under sodium pentobarbital anesthesia (60 mg/kg, i.p.), rats were perfused intracardially with a fixative solution containing 4% paraformaldehyde, 0.1% glutaraldehyde, and 15% picric acid in 0.12 M PB. Brains were then postfixed in the same fixative for 1 hour at RT and rinsed in 0.12 M PB for 1.5 hours. Vibratome sections (80 μm thick) were coronally cut and rinsed in 0.12 M PB. The sections were osmicated (1% osmium in PB) for 1 hour, rinsed, dehydrated in ethanol, counterstained with uranyl (1% uranyl acetate was added at the 70% ethanol stage for 40 minutes), and embedded in Durcupan (ACM, Fluka, Buchs, Switzerland). For each control and pilocarpine-treated animal, four sections were selected at regular intervals beginning at the septal part of the hippocampal formation in which there was a complete typical profile of CA1. The entire width of the CA1 pyramidal cell layer was isolated from each section under a binocular dissecting microscope, reembedded in Durcupan, and sectioned for electron microscopy. Ultrathin serial sections were collected on Formvar-coated single-slot grids, stained with lead citrate, and examined with a Hitachi 7100 electron microscope.

Quantification of the synaptic density and synaptic coverage. Samples for the quantification of the synaptic density and synaptic coverage of the axon initial segments (AIS) of CA1 pyramidal cells was obtained from three control and three pilocarpine-treated rats according to well-established criteria (Wittner et al., 2002). These features include the electron-dense undercoating of the axolemma, the organization of microtubules into fascicles, and the frequent occurrence of lamellar bodies (for review, see Peters et al., 1991). The entire pyramidal cell layer and the proximal half of stratum oriens was systematically scanned and all AISs were digitized; thus, there was no bias for sampling more proximal or distal AISs. To avoid repeated sampling of the same synapses in serial sections, only every tenth section was scanned; digitization was performed using a MegaView II CCD camera and the AnalySIS 3.1 software. The perimeters of the AISs and the length of the synapses they receive were measured by means of the NIH Image program. For each control and epileptic rat, the number and the length of synapses were summed; each of these numbers was divided by the sum of AIS perimeters in order to obtain, respectively, the synaptic density (number of synapses per 100 μm perimeter of AIS) and the synaptic coverage (μm synaptic length per 100 μm perimeter of AIS). All synapses analyzed in this study corresponded to symmetric synapses. Asymmetric synapses were not observed on the AIS of CA1 pyramidal cells from control as well as pilocarpine-treated animals.

RESULTS

Total number of neurons lost in pilocarpine-treated animals with spontaneous seizures

Cresyl violet staining and immunohistochemical counterstaining for NeuN, performed in all sections labeled for GAD65 mRNA and somatostatin, were used to identify the regions of neuronal loss in the hippocampal formation of pilocarpine-treated rats as compared to control animals. In the CA1 region of pilocarpine-treated animals with spontaneous recurrent seizures, a clear loss of cell bodies labeled with cresyl violet (Fig. 1) or NeuN (Fig. 2) was observed in the stratum oriens. This cell loss contrasted with the relative preservation of the pyramidal cells and neurons scattered in stratum radiatum and stratum lacunosum-moleculare (Fig. 1). This observation was confirmed by quantitative analysis showing a 51% decrease in the total number of neurons labeled for NeuN in the stratum oriens/alveus from pilocarpine-treated rats (mean ± SEM number of neurons, 7,712 ± 382; range, 6,984–8,832 in control, and 3,803 ± 332; range, 2,916–4,800 in pilocarpine rats; $P < 0.002$) (Fig. 3). No significant difference in the total number of neurons was observed between control and pilocarpine-treated rats in stratum radiatum/lacunosum-moleculare (7,724 ± 392; range, 6,708–9,336 for control and 8,807 ± 228; range, 8,618–9,372 for pilocarpine rats; Fig. 3).

Loss of GAD-containing neurons in the stratum oriens of CA1

In control animals, many GAD-containing neurons labeled for GAD67 (Fig. 2A) or GAD65 mRNA (Fig. 2C) were distributed in all layers of CA1, as previously described (Houser and Esclapez, 1994; Esclapez and Houser, 1999). In pilocarpine-treated rats, many neurons labeled for GAD mRNA (Fig. 2D) and protein (Fig. 2B) were observed in stratum radiatum/lacunosum-moleculare and stratum pyramidale. Despite some differences (a decrease in stratum pyramidale and an increase in stratum radiatum/lacunosum-moleculare), the mean numbers of GAD mRNA-labeled neurons in these layers were not significantly different in control and epileptic animals (3,644 ± 373; range, 3,096–4,356 for control and 2,460 ± 292; range, 2,052–3,136 for epileptic rats in stratum pyramidal; 6,580 ± 524; range, 5,532–7,116 for control, and 7,770 ± 256; range, 7,272–8,460 for epileptic animals, in stratum radiatum/lacunosum-moleculare). These data likely reflected slight changes in laminar distributions of GAD mRNA-containing neurons located along the border of strata pyramidale and radiatum in control versus pilocarpine-treated animals, since the total numbers of GAD mRNA-labeled neurons in these two layers (strata pyramidale + radiatum/lacunosum-moleculare) were similar in the two animal groups (10,224 ± 198; range 9,888–10,572 for control and 10,230 ± 200; range, 9,696–10,560

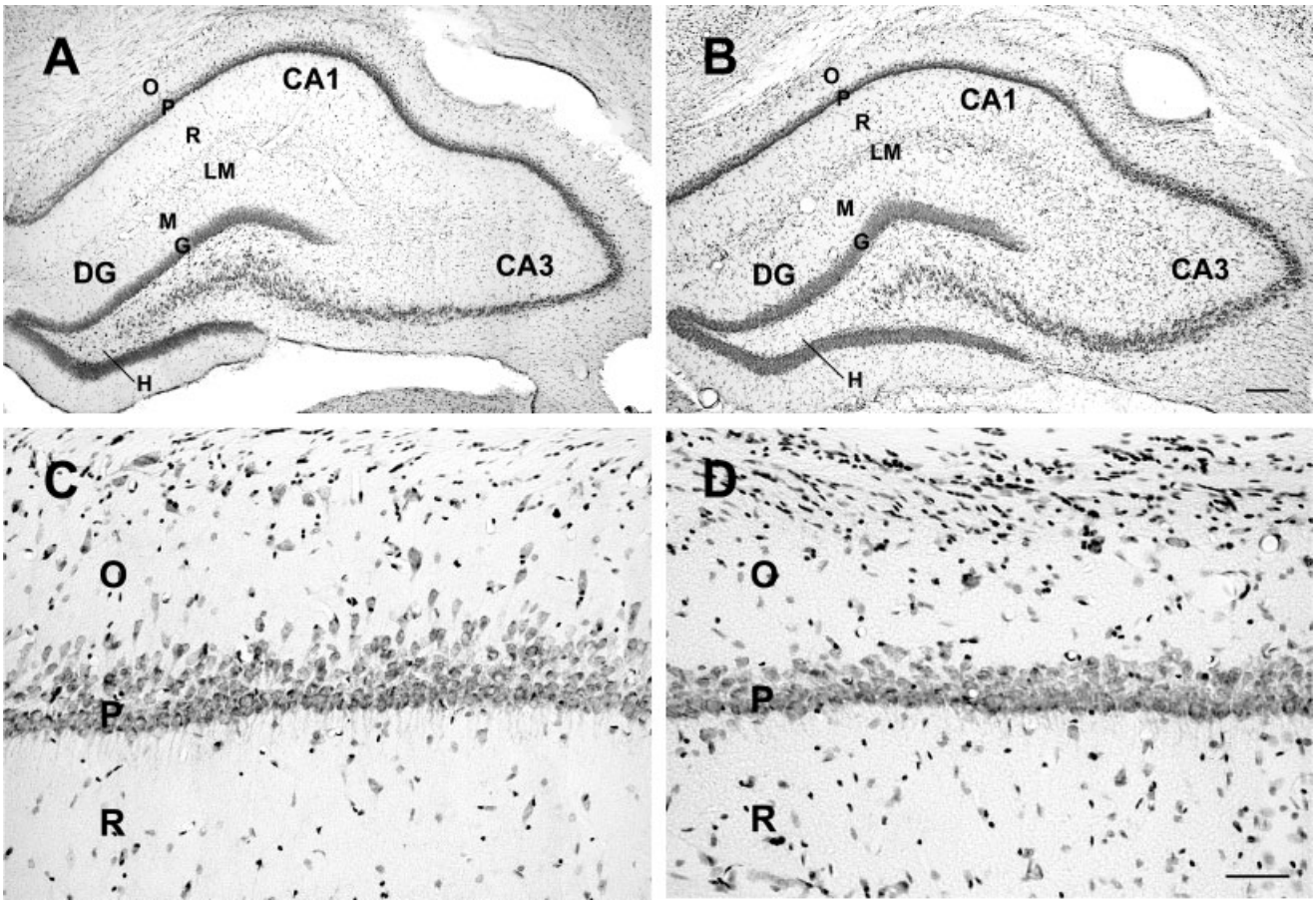

Fig. 1. Cresyl violet-stained sections of the hippocampal formation of (**A,C**) control and (**B,D**) pilocarpine-treated rats. **A:** In a control animal, the cell bodies of principal cells are highly concentrated and form a continuous band in the pyramidal cell layer (P) of the CA3 and CA1 regions and in the granule cell layer (G) of the dentate gyrus. Many neurons are distributed in all other layers including the stratum oriens (O), stratum radiatum (R), and stratum lacunosum-moleculare (LM) of CA1 as well as the stratum moleculare (M) and hilus (H) of dentate gyrus (DG). **B:** In a pilocarpine-treated rat with spontaneous seizures, the number of neurons is reduced in the stratum oriens of CA1 and in the hilus of the dentate gyrus (compare **B** with **A**). A slight neuronal loss is also observed in some regions of CA3, whereas the CA1 pyramidal cell layer is relatively well-preserved. **C,D:** High-magnification photomicrographs of CA1 stratum oriens layers from the same specimens illustrated in **A** and **B**. In this layer, whereas many neurons are present in (**C**) the control animal, only a few neuronal cell bodies are observed in (**D**) the pilocarpine-treated rat. Scale bars = 200 μm in **A,B,** 50 μm in **C,D.**

for pilocarpine animals). In contrast, a marked (52%) decrease ($P < 0.008$) of neurons labeled for GAD mRNA were observed in the stratum oriens/alveus of pilocarpine-treated animals (2,814 ± 519; 1,656–4,080) as compared to control animals (5,952 ± 515; range, 4,968–6,708) (Fig. 3).

Some neurons single-labeled for NeuN were also observed in stratum oriens and stratum radiatum/lacunosum-moleculare from control and pilocarpine-treated animals (Fig. 2C,D). These non-GABAergic neurons, which could correspond to ectopic pyramidal cells or giant neurons (Gulyas et al., 1998), represented 22% of the neurons in stratum oriens and 13% in stratum radiatum/lacunosum-moleculare in control rats. No statistical difference in the numbers of these non-GABAergic neurons was observed between control and pilocarpine-treated animal in stratum radiatum/lacunosum-moleculare. However, in the stratum oriens of pilocarpine animals the number of neurons only labeled for NeuN (849 ± 81; range, 612–960) was significantly decreased ($P < 0.02$) compared to control rats (1,656 ± 174; range, 1,476–2,004) (Fig. 3).

Therefore, the prominent decrease in the total number of neurons observed in the stratum oriens of CA1 in pilocarpine-treated rats with spontaneous seizures is mainly due to a massive loss of GAD-containing neurons. Despite a decrease of more than 50% in the number of GAD-labeled neurons in stratum oriens, many of these interneurons were preserved in all other layers of CA1. An extensive field of GAD-containing terminals was observed within the pyramidal cell and dendritic layers of the hippocampal formation in control as in pilocarpine-treated rats. The overall laminar patterns of labeling for GAD-containing terminals were similar in pilocarpine-treated and control rats, including the high level of terminal labeling within the pyramidal cell layer (Fig. 2A,B).

Loss of somatostatin-containing neurons in the stratum oriens of CA1

The distribution of somatostatin-containing neurons has been reported previously (Somogyi et al., 1984; Kosaka et al., 1988). Somatostatin-containing neurons are

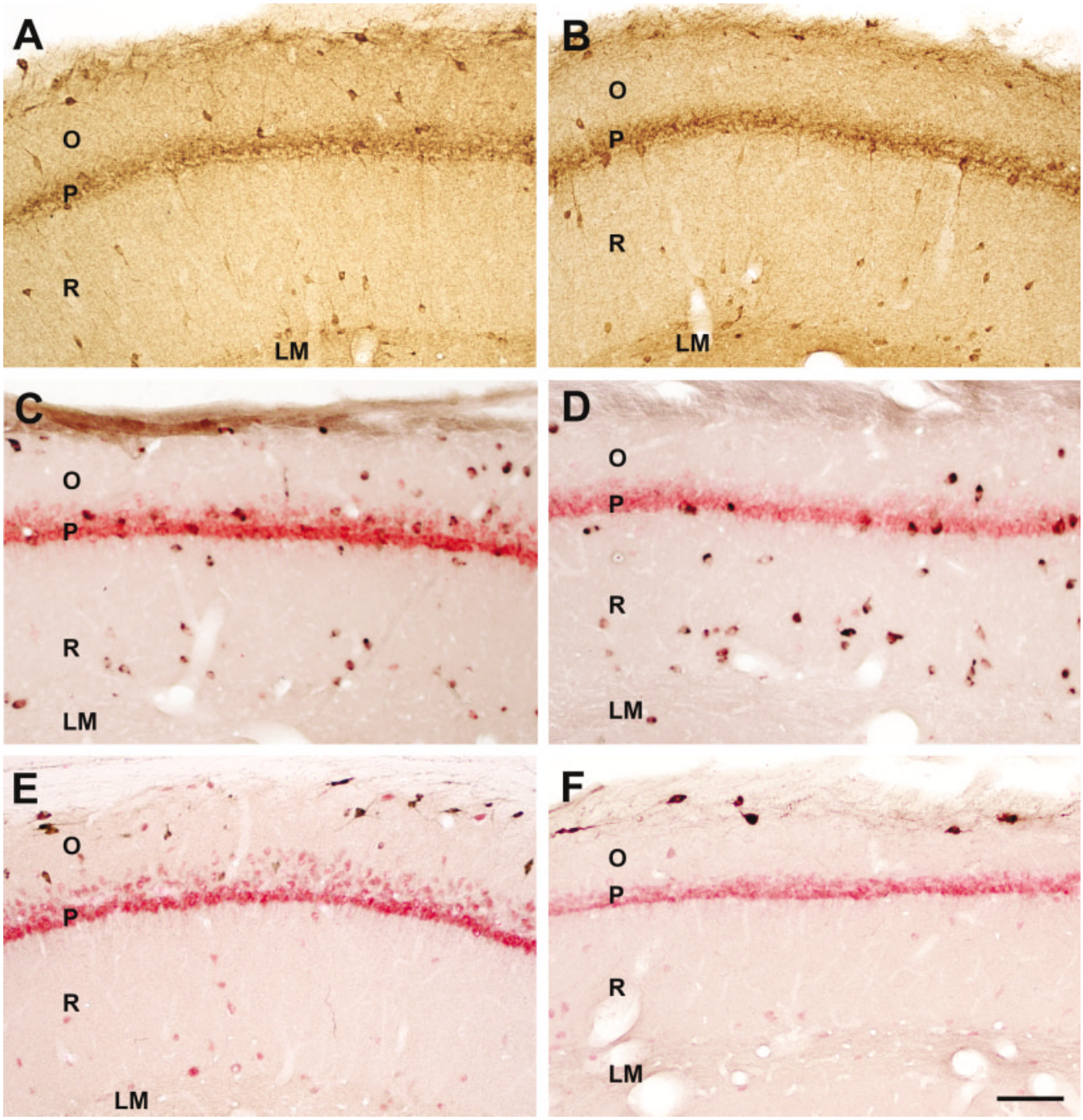

Fig. 2. GAD67-, GAD65 mRNA-, somatostatin-, and NeuN-containing neurons in the CA1 region of the hippocampal formation in (**A,C,D**) control and (**B,D,F**) pilocarpine-treated rats. **A:** In a control rat, the cell bodies of neurons immunolabeled for GAD67 are observed in all layers of CA1 including stratum oriens (O), the pyramidal cell layers (P), stratum radiatum (R), and stratum lacunosum-moleculare (LM). GAD67-immunoreactive terminals are highly concentrated in the stratum pyramidale but are also present in all the dendritic layers of CA1. **B:** In a pilocarpine-treated rat, only a few GAD67-containing neurons are observed in the stratum oriens as compared to (**A**) the control animal, whereas many of these neurons are present in all other layers. The densities of staining for GAD67-containing terminals are similar to those observed in (**A**) the control rat including in the pyramidal cell layer. **C:** In a control rat, many GAD65 mRNA-containing neurons are distributed in all layers of CA1. In the dendritic layers, the majority of NeuN-containing neurons are labeled for GAD65 mRNA; only a few neurons single-labeled for NeuN are observed in stratum oriens and stratum radiatum. **D:** In a pilocarpine-treated rat, a marked reduction in the number of GAD65 mRNA-containing neurons is evident in the stratum oriens (compare **C** with **D**) whereas many GAD65 mRNA-labeled neurons are still present in the pyramidal cell layer, stratum radiatum, and stratum lacunosum-moleculare. **E:** In a control rat, somatostatin-containing neurons are present in the stratum oriens and along the alveus border (**A**). Non-somatostatinergic neurons, both GABAergic and non-GABAergic, only labeled for NeuN, are evident in all layers of CA1. **F:** In a pilocarpine-treated rat, the number of somatostatin-containing neurons is reduced in the stratum oriens as compared to the control animal (**E**); some remaining neurons are located along the alveus border. Scale bar = 100 μm in **A–F**.

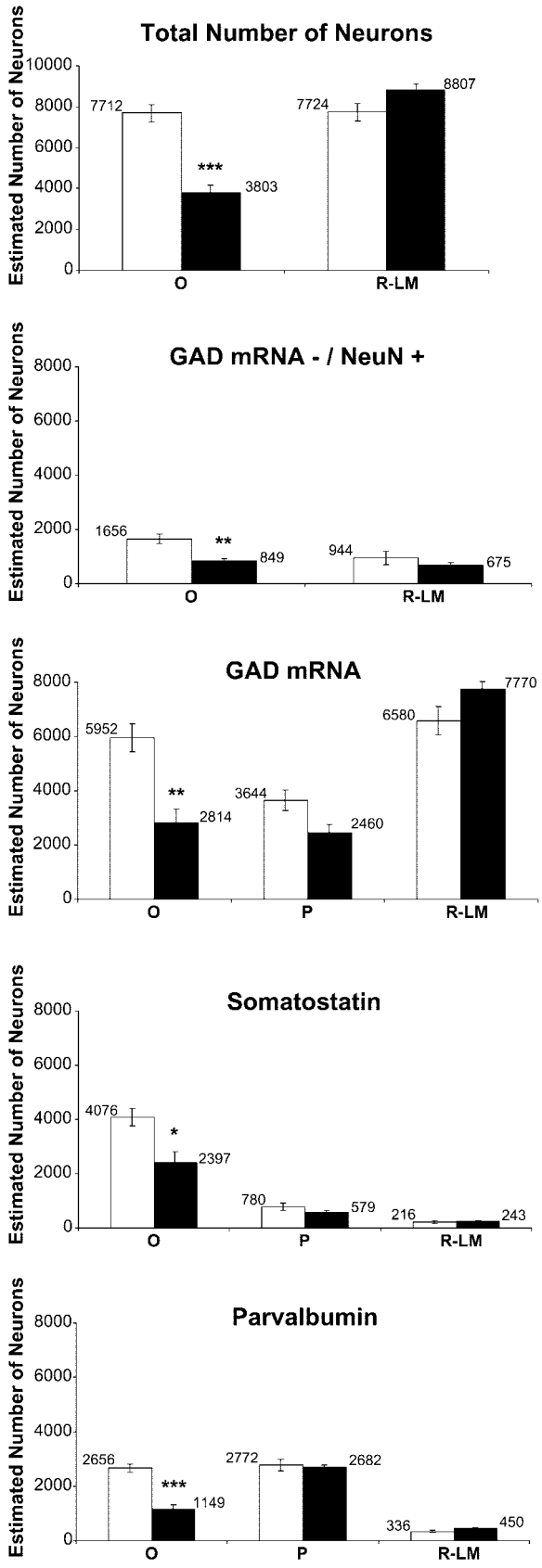

Fig. 3. Bars graphs comparing the mean estimated numbers of NeuN-, GAD mRNA-, somatostatin-, and parvalbumin-containing neurons in control (white bars) and pilocarpine-treated (black bars) animals with spontaneous seizures in the different layers of CA1 including stratum oriens (O), stratum pyramidale (P), and stratum radiatum/lacunosum-moleculare (R-LM). Statistically significant differences in the mean estimated number of labeled neurons are indicated (*$P < 0.03$; **$P < 0.02$; ***$P < 0.002$; Student's t-test). Error bars indicate SEM.

one of the major subpopulations of GABA neurons in the stratum oriens of CA1. In control rats, somatostatin-immunoreactive neurons (SS-IR) were located primarily in the stratum oriens and along the alveus/oriens border (Fig. 2E). These interneurons were rarely observed in the pyramidal cell layer or stratum radiatum/lacunosum-moleculare. Pilocarpine-treated rats displayed only few SS-IR neurons in CA1 (Fig. 2F). A marked decrease of labeled neurons (42%) was observed in stratum oriens/alveus as compared to control animals. The mean numbers of labeled neurons were 2,397 ± 426 (range, 1,452–3,432) in pilocarpine versus 4,076 ± 327 (range, 3,516–4,644) in control rats ($P < 0.03$). In contrast, the mean numbers of somatostatin-labeled neurons were similar in control and epileptic animals in stratum pyramidale (780 ± 132; range, 528–940 for control and 579 ± 69; range, 408–744 for pilocarpine rats) and stratum radiatum/lacunosum-moleculare (216 ± 59; range, 108–312 for control and 243 ± 37; range, 144–312 for pilocarpine rats) (Fig. 3).

In sections simultaneously labeled for somatostatin and NeuN from control and pilocarpine-treated rats, many neurons single-labeled for NeuN (both non-GABAergic and GABAergic neurons) were distributed in all layers of CA1 (Fig. 2E,F). A marked decrease in the total number of neurons only labeled for NeuN (59%, $P < 0.003$) was observed in the stratum oriens of pilocarpine-treated rats (1,545 ± 134; range, 1,404–1,944) as compared to control animals (3,740 ± 226; range, 3,468–4,188). In contrast, no significant difference was observed in the stratum radiatum/lacunosum-moleculare (8,925 ± 309; range, 8,388–9,732 for control and 7,708 ± 739; range, 6,600–9,108 for pilocarpine rats) (Fig. 3).

Thus, somatostatin-containing neurons contributed a large part of the loss of GABAergic neurons observed in the stratum oriens of CA1 in pilocarpine-treated animals with spontaneous seizures. However, single labeling for NeuN suggested that other subpopulations of GABAergic neurons were also involved in this neuronal loss.

Loss of parvalbumin-containing neurons in the stratum oriens of CA1

In control animals, the cell bodies of practically all parvalbumin-containing neurons in CA1 were located in the pyramidal cell layer and in stratum oriens, as previously described (Kosaka et al., 1987). Somata labeled for parvalbumin were extremely rare in the stratum radiatum/lacunosum-moleculare of CA1 and, when present, these cells were mostly located close to the pyramidal cell layer (Fig. 4A). The dendrites of parvalbumin-containing neurons extended through all dendritic layers, becoming relatively sparse in stratum lacunosum-moleculare (Fig. 4A). Parvalbumin-immunoreactive (PV-IR) terminals were concentrated mainly

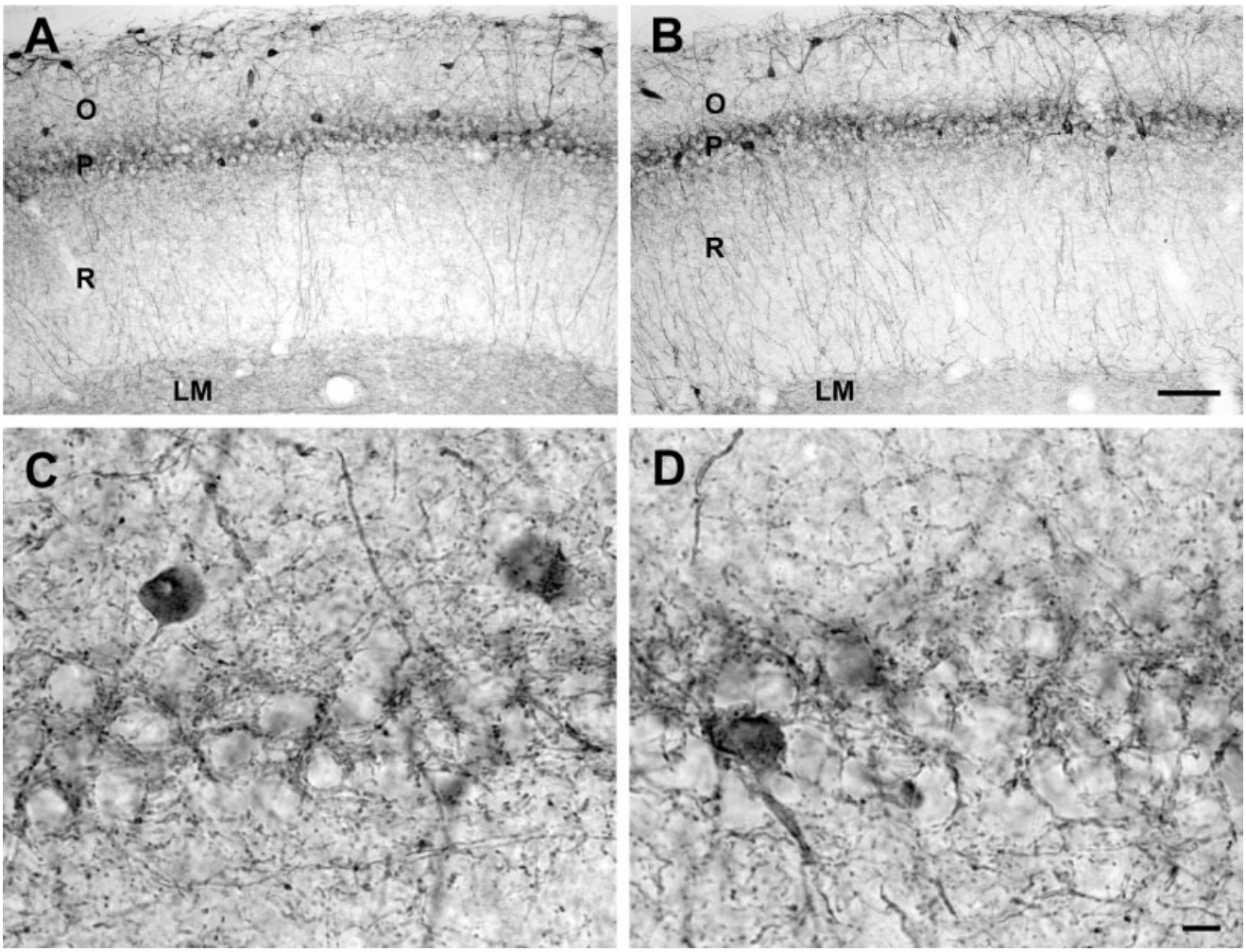

Fig. 4. Comparison of immunohistochemical labeling for parvalbumin in the CA1 region of the hippocampal formation from (**A,C**) control and (**B,D**) pilocarpine-treated rats. **A:** In a control rat, the cell bodies of parvalbumin-containing neurons are mainly concentrated in the pyramidal cell layer (P) but are also located in the stratum oriens (O). High densities of parvalbumin-immunoreactive terminals are observed in the pyramidal cell layer, proximal stratum oriens, and stratum radiatum (R). **B:** In a pilocarpine-treated rat with spontaneous seizures, very few cell bodies immunoreactive for parvalbumin are present in the stratum oriens, whereas many neurons and terminals are still observed in the pyramidal cell layer. **C,D:** High-magnification photomicrographs of CA1 stratum pyramidale in (**C**) control and (**D**) pilocarpine-treated animals. Many parvalbumin-containing terminals surrounding the cell bodies of unlabeled pyramidal cells are observed in control as well as in pilocarpine treated animals. Scale bars = 100 μm in **A,B,** 10 μm in **C,D.**

in the pyramidal cell layer and proximal stratum oriens and stratum radiatum (Fig. 4C). These terminals labeled for parvalbumin surrounded the cell bodies (Fig. 4C) and axon initial segments of pyramidal cells, as previously described (Kosaka et al., 1987; Katsumaru et al., 1988).

In pilocarpine-treated animals, a marked decrease in parvalbumin-labeled neurons was observed in the stratum oriens of CA1 (Fig. 4B). This decrease was further confirmed by the quantitative analysis showing a 57% drop in the mean number of PV-IR neurons (2,656 ± 154; range, 2,484–2,964 for control and 1,149 ± 158; range, 828–1,560 for pilocarpine-treated rats; $P < 0.001$). No significant difference was observed in the pyramidal cell layer or stratum radiatum/lacunosum-moleculare between control and pilocarpine animals. The mean numbers of PV-IR interneurons were 2,772 ± 211 (range, 2,532–3,192) for control and 2,682 ± 85 (range, 2,532–2,928) for pilocarpine animals in the pyramidal cell layer, and 336 ± 37 (range, 312–408) for control and 450 ± 37 (range, 396–552) for pilocarpine rats in the stratum radiatum/lacunosum-moleculare (Fig. 3). Despite the clear loss of parvalbumin-containing neurons in the stratum oriens of CA1, the general laminar pattern of labeling for parvalbumin-containing terminals was similar in pilocarpine-treated and control rats, including the high level of terminal labeling within the pyramidal cell layer (Fig. 4B,D).

Thus, in animals with spontaneous limbic seizures parvalbumin- and somatostatin-containing neurons contributed to the cell loss of GABAergic neurons in stratum oriens of CA1.

Subpopulation of neurons containing both somatostatin and parvalbumin

The patterns of distribution as well as the numbers of SS- and PV-IR neurons were similar in sections processed

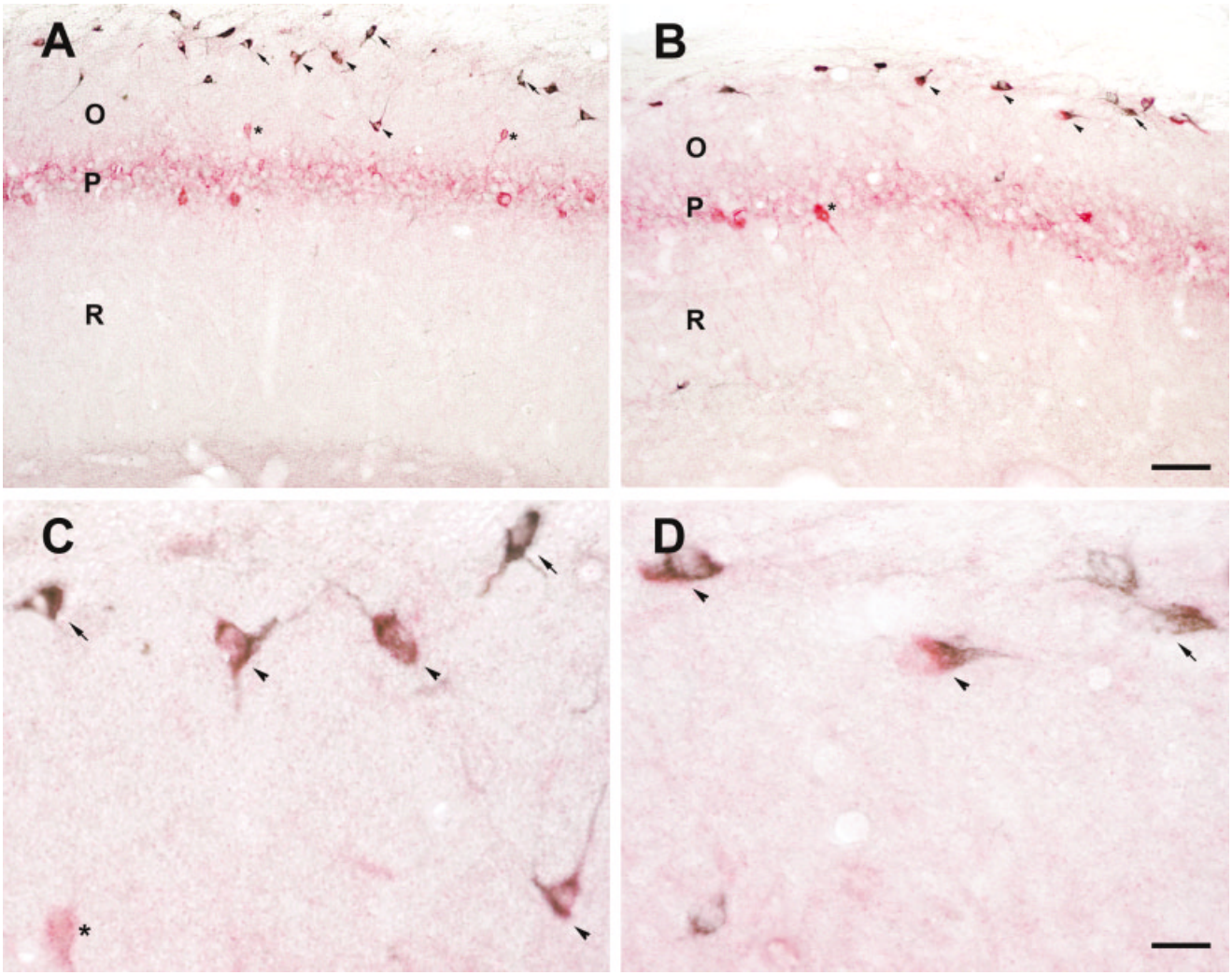

Fig. 5. Comparison of double immunohistochemical labeling for somatostatin/parvalbumin in the CA1 region of the hippocampal formation from (**A,C**) control and (**B,D**) pilocarpine-treated rats. **A:** In the stratum oriens (O) of a control rat, many neurons double-labeled for somatostatin and parvalbumin (arrow heads) are observed in addition to neurons only labeled for somatostatin (arrows, dark blue) or for parvalbumin (*, red). In the pyramidal cell layer (P), neurons are only labeled for parvalbumin. **B:** In the stratum oriens of pilocarpine-treated rat, the numbers of neurons only labeled for somatostatin or for parvalbumin are decreased as compared to the control rat (**A**), whereas many neurons double-labeled for somatostatin and parvalbumin are still observed. **C,D:** High-magnification photomicrographs of stratum oriens (O) in (**C**) control and (**D**) pilocarpine-treated animals illustrate double- and single-labeled neurons for somatostatin (dark blue) and parvalbumin (red). Scale bars = 100 μm in **A,B,** 25 μm in **C,D.**

for double and for single labeling (Fig. 5). In the CA1 region of control rats, neurons containing both somatostatin and parvalbumin were located mainly in the stratum oriens; only a few double-labeled neurons were observed in stratum pyramidale (Fig. 5A,C). The average estimated number of double-labeled neurons was 736 ± 32 in the stratum oriens of CA1. These neurons represented 15% of the SS-IR neurons and 44% of the PV-IR neurons located in this layer (Fig. 6). In pilocarpine-treated animals, a marked decrease in the number of neurons was observed in the stratum oriens of CA1 for neurons only labeled for somatostatin (42%; 2,512 ± 81; range, 2,352–2,616 in pilocarpine as compared to 4,316 ± 73; range, 4,200–4,452 in control rats, $P < 0.0001$), and neurons only labeled for parvalbumin (34%; 628 ± 58; range, 516–708 in pilocarpine as compared to 948 ± 78; range, 864–1,104 in control rats, $P < 0.03$). In contrast, no significant difference in the number of neurons that coexpressed somatostatin and parvalbumin was observed between control and pilocarpine-treated rats (736 ± 32; range, 672–768 for control and 616 ± 83; range, 468–756 for pilocarpine rats) (Figs. 5B,D, 6).

Subpopulation of neurons containing both somatostatin and calbindin

In the CA1 region of control rats, neurons that coexpressed somatostatin and calbindin were located in the stratum oriens (Fig. 7A,C). The average estimated number of these neurons was 576 ± 84 in the stratum oriens of CA1 and represented 11% of the somatostatin-containing

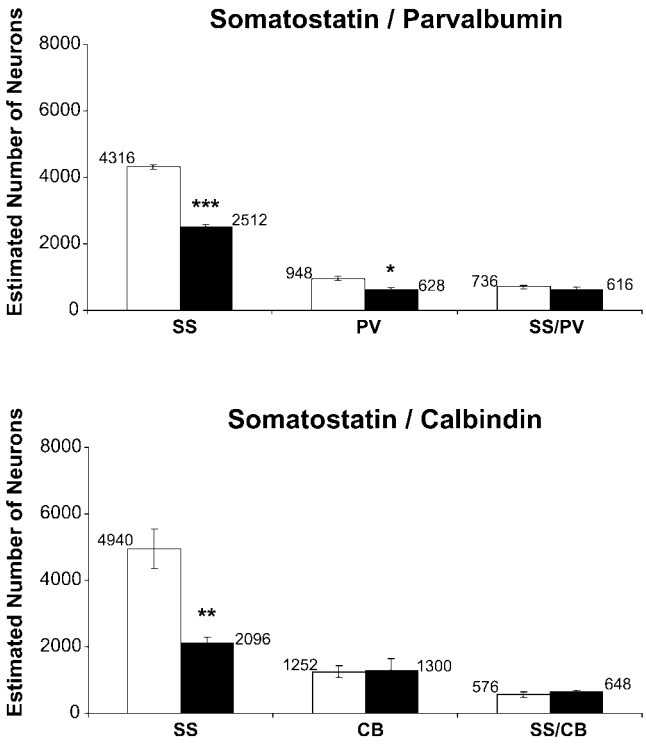

Fig. 6. Bar graphs comparing the mean estimated numbers of neurons only labeled for somatostatin (SS), parvalbumin (PV), or calbindin (CB) and neurons that coexpress somatostatin/parvalbumin (SS/PV) or somatostatin/calbindin (SS/CB) in the CA1 stratum oriens of control (white bars) and pilocarpine-treated (black bars) rats with spontaneous seizures. Statistically significant differences in the mean estimated number of labeled neurons are indicated (*$P < 0.03$; **$P < 0.001$; ***$P < 0.0001$; Student's t-test). Error bars indicate SEM.

neurons located in this layer (Fig. 6). In pilocarpine-treated animals, whereas the number of SS-IR neurons that did not contain calbindin was strongly decreased (58%; 2,096 ± 197; range, 1,764–2,448 in pilocarpine as compared to 4940 ± 580; range, 3,792–5,748 in control rats; $P < 0.001$), the numbers of neurons that coexpressed somatostatin and calbindin (576 ± 84; range, 480–744 in control and 648 ± 60; range, 528–720 in pilocarpine rats) or were only labeled for calbindin (1,252 ± 177; range, 960–1,572 in control and 1,300 ± 346; range, 924–1,992 in pilocarpine rats) were not significantly different from those observed in control animals (Figs. 6, 7B,D).

To summarize, quantitative analyses of double-labeling experiments indicated that the large and consistent decrease in the numbers of SS- and PV-IR neurons within the stratum oriens of CA1 consisted only of neurons labeled for somatostatin or parvalbumin, but not neurons labeled for both, nor somatostatin-containing neurons that coexpressed calbindin.

Neuroanatomical changes at 72 hours, 1 and 2 weeks after pilocarpine injection

Data from neurodegenerative and immunohistochemical studies were obtained from the same control and pilocarpine-treated animals. Labeling for neuronal degeneration with the Gallyas and fluoro-jade B methods (Fig. 8) revealed, respectively, darkly labeled and fluorescent neurons in the stratum oriens of pilocarpine-treated animals at each time interval after status epilepticus induction (Fig. 8A,B). In addition, many darkly labeled or fluorescent punctiform elements, presumed to be degenerating axon terminals and fibers, were evident at 1 and 2 weeks in the stratum lacunosum-moleculare (Fig. 8A,C), the stratum oriens, as well as at the border of strata pyramidale and proximal oriens (Fig. 8B). Adjacent sections performed for immunohistochemical localization of somatostatin and parvalbumin showed a marked decrease in the numbers of SS- and PV-IR neurons in the stratum oriens of pilocarpine-treated animals at each time interval after pilocarpine treatment. Quantitative analysis showed significant differences in the mean number of SS- and of PV-IR neurons between control and pilocarpine-treated animals at each interval (Fig. 9). In the stratum oriens of CA1, marked decreases in SS-IR neurons were observed at 72-hour (38%), 1-week (48%), and 2-week (41%) intervals. Similar reductions in the number of PV-IR neurons were observed at 72 hours (53%), 1 week (55%), and 2 weeks (54%). These differences between control and pilocarpine-treated animals were statistically significant ($P < 0.001$) for all intervals. No significant difference in mean numbers of SS- or PV-IR neurons in the stratum oriens of pilocarpine-treated rats was observed between the different groups (72 hours, 1 week, and 2 weeks) and the animals with spontaneous seizures (3 months after pilocarpine treatment). Therefore, the large decreases in SS- and PV-IR neurons observed in epileptic animals occurred as soon as 72 hours after pilocarpine treatment and were associated with neuronal degeneration.

Synaptic coverage of axon initial segment of CA1 pyramidal cells

We examined whether the decrease in the number of stratum oriens interneurons containing parvalbumin only, corresponds to a loss of axo-axonic cells. The synaptic coverage and the density of synaptic inputs of axon initial segments (AIS) of CA1 pyramidal cells were analyzed.

Symmetrical synapses on AIS were present in control and pilocarpine-treated animals (Fig. 10). However, these synapses were more frequently observed along the AIS in control than in pilocarpine-treated rats (Fig. 10A,B). Quantitative analysis of data obtained in each animal is reported in Table 2; this demonstrates a clear decrease in the synaptic density (SDen) (63%, $P < 0.00001$) and in the synaptic coverage (SCov) (63%, $P < 0.00001$) of symmetrical synapses on the AIS in pilocarpine-treated rats (mean SDen = 8.2 ± 0.56; mean SCov = 2.2 ± 0.04) as compared to control animals (mean SDen = 21.9 ± 3.2; mean SCov = 6.1 ± 1.15), whereas the average synaptic lengths in the six animals did not differ significantly (Table 2). Thus, in pilocarpine-treated animals with spontaneous limbic seizures, CA1 pyramidal cells displayed a clear decrease in the total number of symmetrical synapses on their axon initial segments.

DISCUSSION

Previous studies have reported the vulnerability of GABAergic interneurons in the stratum oriens of the CA1 region in the pilocarpine model of temporal lobe epilepsy (TLE) (Houser and Esclapez, 1996; Cossart et al., 2001; Andre et al., 2001). The present findings confirm these observations and further demonstrate that this loss is

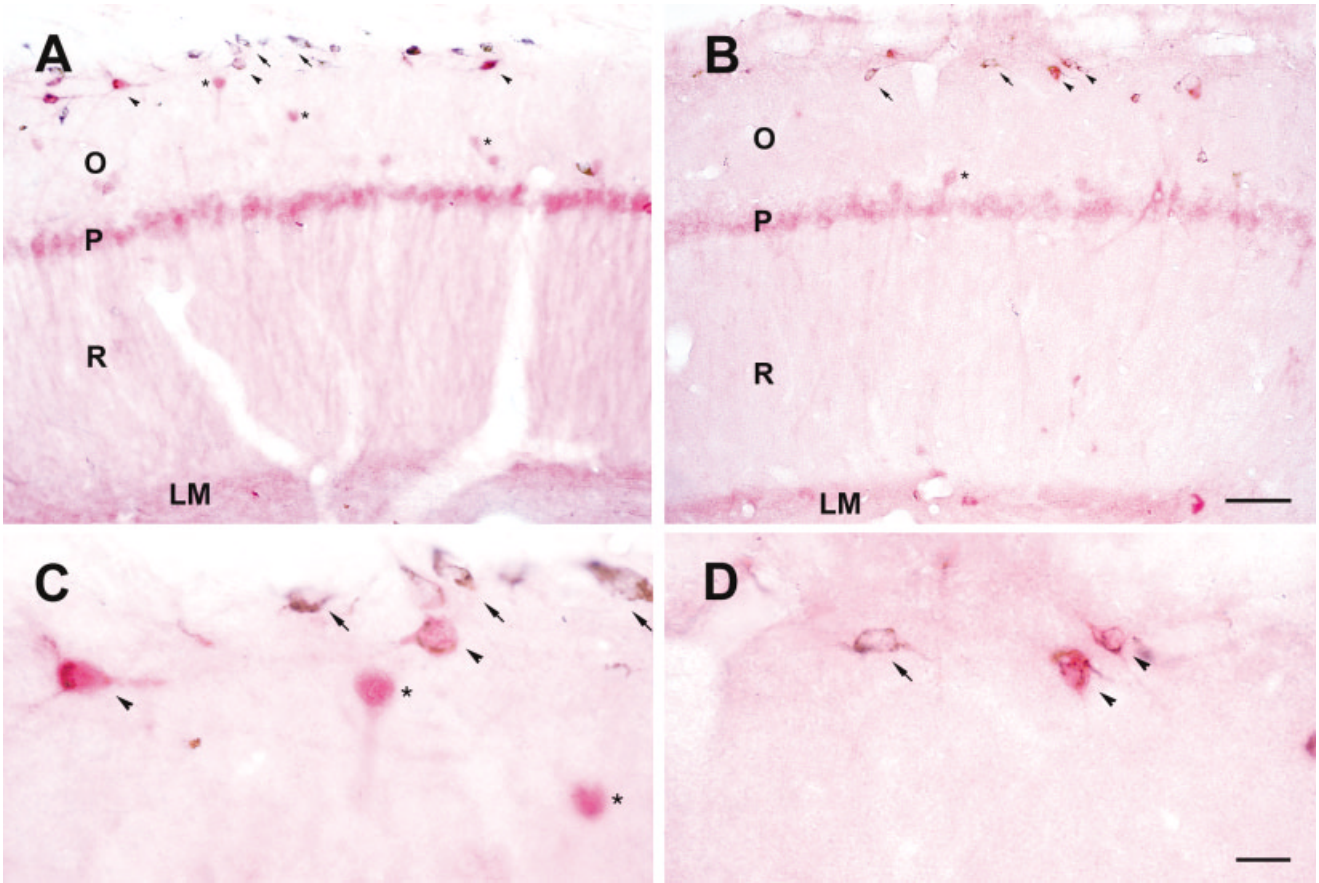

Fig. 7. Comparison of double immunohistochemical labeling for somatostatin/calbindin in the CA1 region of the hippocampal formation from (**A,C**) control and (**B,D**) pilocarpine-treated rats. **A–D:** Simultaneous detection of somatostatin and calbindin neurons shows that many remaining somatostatin-containing neurons in the stratum oriens of pilocarpine-treated animals (**C,D**) coexpress calbindin. Neurons only labeled for somatostatin (arrows), calbindin (*), and neurons that coexpress somatostatin/calbindin (arrow heads). Scale bars = 100 μm in **A,B,** 25 μm in **C,D.**

almost completely due to the death of two specific subpopulations of stratum oriens GABAergic interneurons identified on the basis of their neurochemical and morphological properties, the somatostatin-containing O-LM cells and parvalbumin-containing axo-axonic cells. This cell loss contrasts with the preservation of other subpopulations of GABAergic neurons in the stratum oriens as well as all interneurons in the strata pyramidale, radiatum, and lacunosum-moleculare. Furthermore, we have demonstrated that the loss of these subpopulations of somatostatin- and parvalbumin-containing interneurons occurs before the emergence of spontaneous recurrent limbic seizures.

Our data clearly show that pilocarpine-treated animals with spontaneous recurrent seizures display, in the stratum oriens of CA1, a significant reduction in the number of GAD mRNA-containing neurons, a reduction which is associated with major decreases in the numbers of somatostatin- and parvalbumin-containing neurons. Several results in the present study suggest that the decrease in the number of these interneurons reflects neuronal death rather than a downregulation at the mRNA or protein/peptide levels. First, the loss of GABAergic interneurons was associated with a drop in the total number of neurons. A large number of degenerating neurons was observed with the Gallyas and fluoro-jade B methods in the stratum oriens as soon as 72 hours (the shortest survival time examined in this study) after pilocarpine-induced status epilepticus and was still evident at 1 and 2 weeks after injection. Furthermore, this neuronal degeneration was accompanied by the loss of somatostatin- and parvalbumin-containing interneurons as soon as 72 hours after injection. Finally, the percentage of loss was relatively constant at all examined time points and was evident as long as 12 weeks after pilocarpine administration.

In addition, our data show that pilocarpine-treated animals with spontaneous recurrent seizures display no change in the number of interneurons coexpressing somatostatin/parvalbumin and somatostatin/calbindin. Despite the possibility that an upregulation in peptide and/or calcium binding protein expression, in some neurons that in control condition would show no or undetectable levels, might contribute to these preserved-cell numbers, it is more likely that these data reflect the preservation of these two subpopulations of interneurons in epileptic animals.

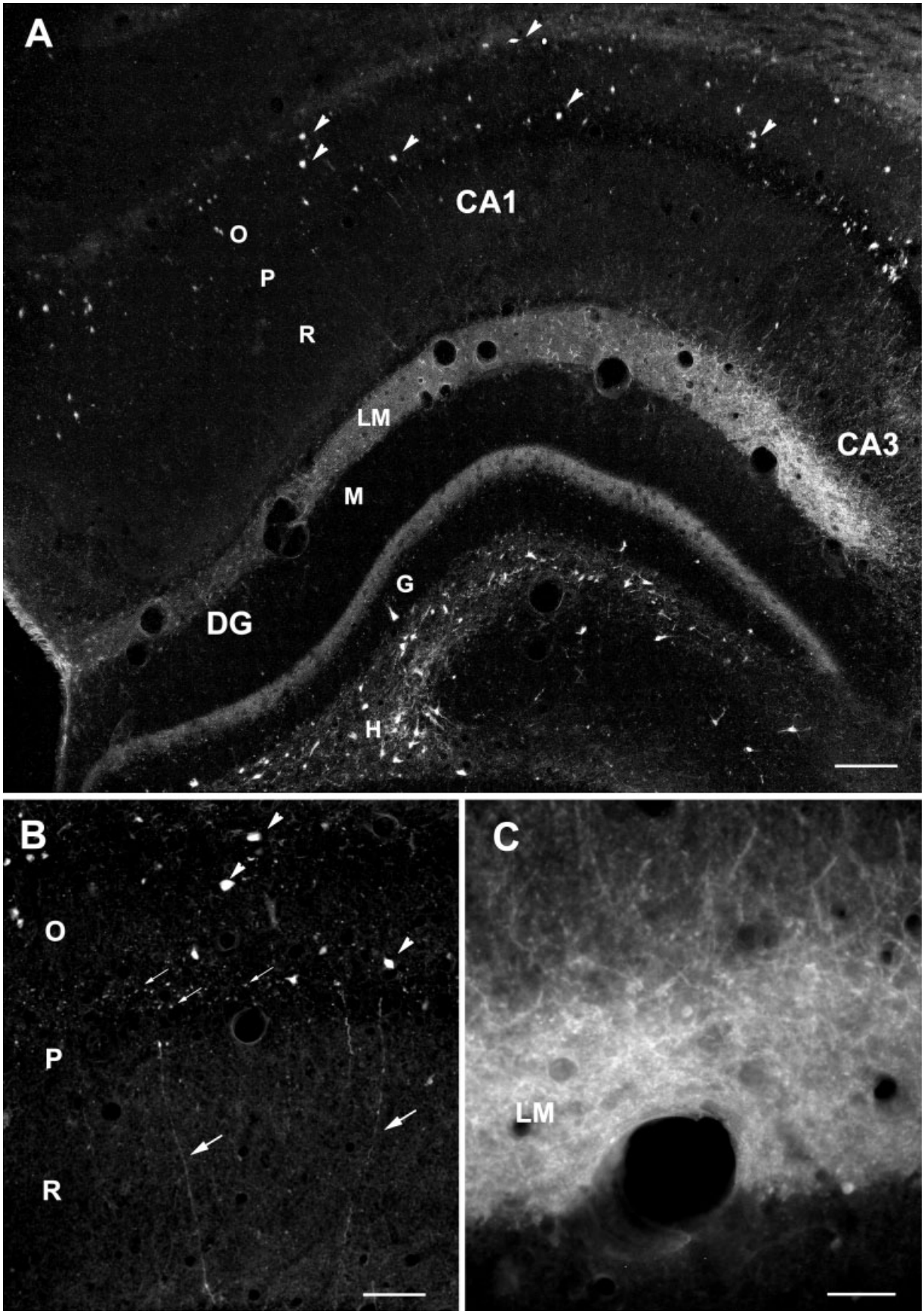

Fig. 8. Neuronal degeneration in the hippocampal formation of a rat, 1 week after pilocarpine treatment. **A:** degenerating neurons (arrow heads) labeled for fluoro-jade-B are present in the stratum oriens (O) and along the alveus border (A) of CA1 as well as in the hilus (H) of the dentate gyrus (DG) and in the stratum pyramidale (P) of CA3. **B,C**: High magnification photomicrographs of the CA1 region illustrated in (**A**). **B**: Some degenerating cell bodies in stratum oriens (arrow heads), degenerating processes (thick arrows) running through stratum radiatum (R) and degenerating terminals (thin arrows) in strata pyramidale and proximal oriens are observed. **C**: Many degenerating axon terminals and fibers are present in the stratum lacunosum-moleculare (LM). Scale bars = 100 μm in **A**, 50 μm in **B**, 25 μm in **C**.

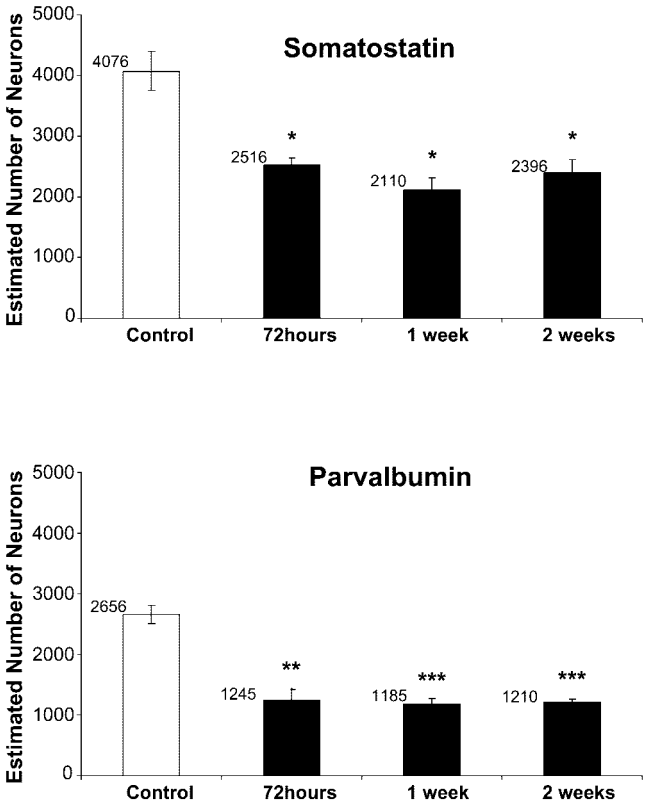

Fig. 9. Bar graphs comparing the mean estimated numbers of somatostatin- and parvalbumin-containing neurons in the CA1 stratum oriens of control (white bars) and pilocarpine-treated (black bars) rats at 72 hours and 1 and 2 weeks following pilocarpine treatment. Statistically significant differences in the mean estimated number of labeled neurons are indicated (*$P < 0.01$, **$P < 0.005$; ***$P < 0.001$; Student's t-test). Error bars indicate SEM.

Loss of somatostatin-containing O-LM cells

Our quantitative stereological study demonstrates the vulnerability of interneurons labeled for somatostatin only in the stratum oriens of CA1 in pilocarpine-treated animals. This result confirms a previous semiquantitative study in this model (Cossart et al., 2001). We have thus demonstrated, in the stratum oriens of animals with chronic limbic seizures a loss of more than 40% of the total number of somatostatin-containing neurons. In addition, our results strongly suggest that this loss accounts for almost half of the GABAergic degenerating neurons in the stratum oriens since quantitative data show that somatostatin interneurons represent about 60% of the total number of GAD mRNA-containing neurons in the stratum oriens of control animals. Furthermore, this study provides additional evidence that one of the main populations of somatostatin-containing neurons, the so-called O-LM cells, degenerates in this model. These stratum oriens interneurons possess an axon that projects to the stratum lacunosum-moleculare (Sik et al., 1995; Freund and Buzsaki, 1996), where they innervate almost exclusively the distal apical dendrite of CA1 pyramidal cells (Katona et al., 1999). The present study clearly shows many degenerating axon fibers in the stratum lacunosum-moleculare at 1 and 2 weeks after pilocarpine injection. These data are in keeping with a loss of symmetrical synapses on dendrites of pyramidal cells described in the stratum lacunosum-moleculare of pilocarpine-treated animals with spontaneous seizures (Cossart et al., 2001). Therefore, these findings confirm that somatostatin-containing O-LM cells represent a particularly vulnerable interneuron type in the pilocarpine model of TLE.

Loss of parvalbumin-containing axo-axonic cells

The present study also demonstrates a marked loss of parvalbumin-containing interneurons in stratum oriens of animals with spontaneous recurrent seizures. Similar results have been reported recently in the lithium–pilocarpine model of TLE (Andre et al., 2001). In addition, we have shown that interneurons containing parvalbumin only are responsible for this cell loss. Furthermore, the quantitative study strongly suggests that this loss accounts, as with the somatostatin-containing neurons, for a large part of the GABAergic neurons that degenerate in the stratum oriens of CA1. The two principal morphological types of parvalbumin-containing interneurons correspond to basket and axo-axonic cells (Katsumaru et al., 1988). Previous reports and the present study suggest that basket cells are apparently undamaged in the CA1 region of pilocarpine-treated animals. Indeed, many GAD- and parvalbumin-containing neurons, as well as axon terminals labeled for GAD and parvalbumin, are well preserved in the CA1 pyramidal cell layer. No modification in the density of GABAergic boutons is observed around cell bodies of CA1 pyramidal cells in pilocarpine-treated rats (Hirsch et al., 1999). In contrast to basket cells, which are probably preserved in this model, parvalbumin-containing axo-axonic cells are apparently vulnerable. We demonstrated that the loss of parvalbumin-containing neurons in the stratum oriens of CA1 occurs with a significant decrease in the synaptic coverage of axon initial segments (AIS) of pyramidal neurons. The decrease of synaptic coverage likely reflects a reduction in the number of inhibitory synaptic boutons on the AIS, since no major difference regarding the length of synapses has been observed between control and pilocarpine-treated animals. In addition, profiles of degenerating axons terminals were also observed at 1 and 2 weeks after pilocarpine injection in strata pyramidale and proximal oriens, where the axon of axo-axonic cells forms a dense arbor (Li et al., 1992; Freund and Buzsaki, 1996). Therefore, all these results strongly suggest that, in pilocarpine-treated animals with spontaneous seizures, many parvalbumin-containing axo-axonic cells degenerate in CA1. Interestingly, a loss of axo-axonic cells (Chandelier cell) has been described in human epileptic neocortex (Marco et al., 1996,1997; DeFelipe, 1999), whereas a recent study reports that axo-axonic cell terminals on dentate granule cells are preserved in patients with intractable TLE (Wittner et al., 2001). All these data suggest that parvalbumin-containing axo-axonic cells innervating pyramidal cells could display differential vulnerability to excitotoxic damage than those innervating dentate granule cells.

Differential vulnerability among GABAergic neurons

While the vulnerability of some specific groups of GABAergic interneurons, including somatostatin-containing O-LM and parvalbumin-containing axo-axonic cells, is evident in

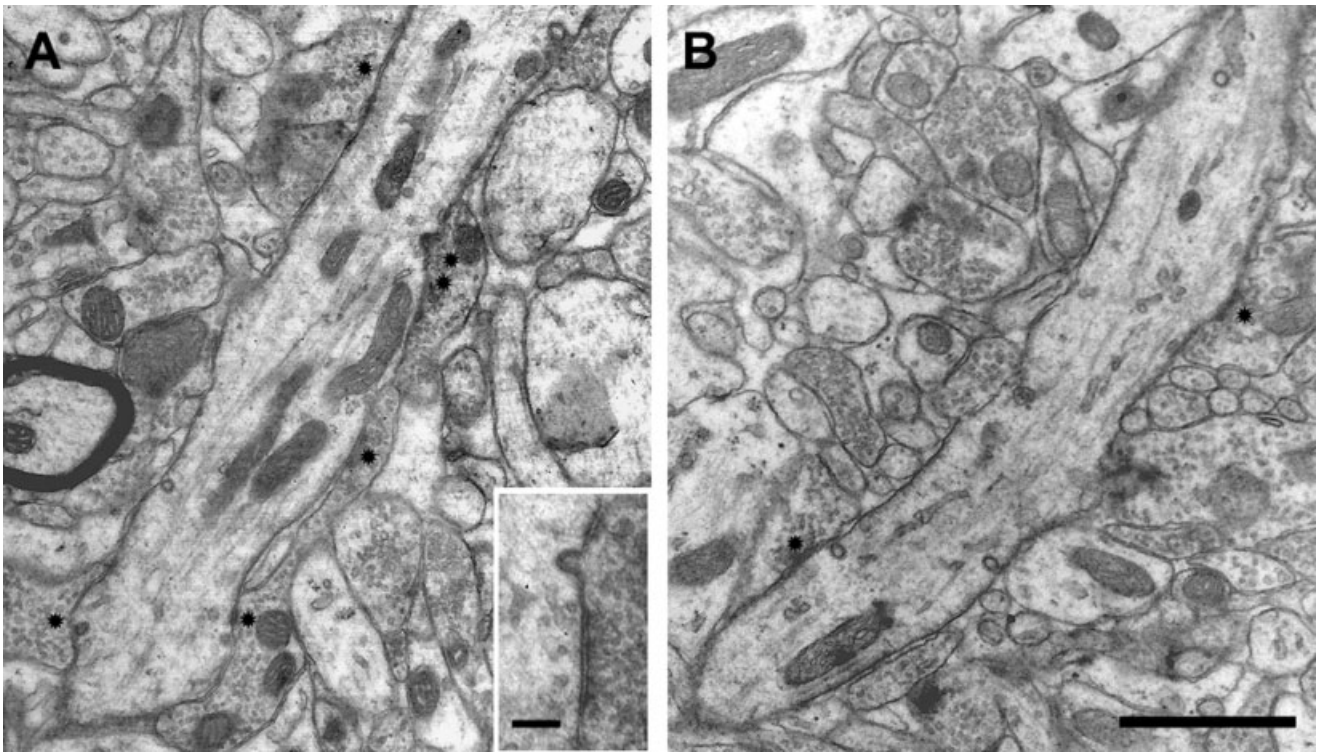

Fig. 10. Synaptic coverage of the axon initial segments of CA1 pyramidal cells in (**A**) control and (**B**) pilocarpine-treated rats. **A:** In a control rat, many axon terminals form symmetrical synapses (*) on the axon initial segment (AIS). Insert: High magnification photomicrograph of one of the symmetrical synapse (**). **B:** In a pilocarpine-treated rat with spontaneous seizures, only few symmetrical synapses are observed along the AIS. Scale bar = 1 μm in **A,B,** 0.5 μm in insert.

TABLE 2. Synaptic Coverage and Density of Axon Initial Segments of CA1 Pyramidal Cells

	Average synaptic coverage (μm active zone/100 μm of AIS perimeter)	Average synaptic density (number of synapses/100 μm of AIS perimeter)	Average synaptic length
control 1	6.87	24.5	0.29
control 2	7.61	25.7	0.3
control 3	3.85	15.6	0.25
pilo 1	2.65	9.18	0.29
pilo 2	2.73	10.3	0.27
pilo 3	1.34	5.24	0.25

the CA1 region of pilocarpine-treated animals, other interneurons are preserved in this region. This differential vulnerability exists even among GABAergic neurons that belong to the same layer; in the stratum oriens, many neurons survive excitotoxic damage, including interneurons coexpressing somatostatin/parvalbumin and somatostatin/calbindin.

The preservation of interneurons containing both somatostatin and parvalbumin has also been described after cerebral ischemia (Bering et al., 1995). These somatostatin/parvalbumin interneurons have been identified recently as O-LM and bistratified cells (Maccaferri et al., 2000; for review, see McBain and Fisahn, 2001). From the study of Maccaferri et al. it is difficult to evaluate the percentage of O-LM and bistratified cells that coexpress somatostatin and parvalbumin, because of the low number of identified neurons tested for their neurochemical content. Nevertheless, a recent study (Pawelzik et al., 2002) shows that a large proportion of bistratified cells contains parvalbumin. These data suggest that many interneurons containing both somatostatin and parvalbumin correspond to bistratified cells. Thus, in pilocarpine-treated animals, bistratified cells are likely preserved. This hypothesis is further supported by our data showing no obvious degenerating axon terminals in stratum radiatum at any of the time points studied after pilocarpine treatment.

According to our findings, stratum oriens interneurons expressing both somatostatin and calbindin are also well-preserved in this model. However, the present results apparently do not confirm recent data describing a loss of calbindin neurons in the CA1 stratum oriens of lithium–pilocarpine-treated animals (Andre et al., 2001). Such an apparent discrepancy between the two studies could be due to the different quantitative analysis used. While our data compare total numbers of neurons estimated using unbiased stereological methods (West et al., 1991; West, 1999), their results compare neuronal densities, relative values that are volume-dependent. Somatostatin/calbindin interneurons are known to project to the medial septum (Toth and Freund, 1992) and were shown recently to display local axonal collaterals that specifically innervate interneurons in CA1 and CA3 (Gulyas et al., 2001). Our results show that this class of interneuron-selective interneurons in CA1 is well-preserved in the pilocarpine model of TLE, as are the vast majority of interneuron-selective interneurons present in strata radiatum and lacunosum-moleculare.

Finally, our data clearly show differential vulnerability of GABAergic neurons among the layers of CA1. Thus, the loss of GABAergic interneurons is restricted to the stratum oriens. All interneurons in the strata pyramidale, radiatum, and lacunosum-moleculare are well preserved, since no difference in the numbers of GAD mRNA-containing neurons or in any subpopulations studied was observed between control and pilocarpine-treated animals. This selective vulnerability of stratum oriens GABAergic interneurons is consistent with previous results in pilocarpine- (Houser and Esclapez, 1996; Andre et al., 2001) and kainic acid-treated models (Morin et al., 1998).

Reasons for such differential vulnerability to excitotoxic damage among GABAergic neurons are unknown. The present study confirms the lack of a direct correlation between the presence or absence of calcium-binding proteins (calbindin or parvalbumin) and interneuron vulnerability to excitotoxic damage as shown in previous studies (Freund et al., 1990,1991; for review, see Freund and Buzsaki, 1996; Houser and Esclapez, 1996). One of the factors that could influence the susceptibility of interneurons to excitotoxic damage is the type and the strength of afferent inputs received by the different types of interneurons. Interestingly, a recent study demonstrates a much higher density of inputs as well as total number of excitatory and inhibitory synapses on parvalbumin- than on calbindin- or calretinin-containing neurons. In addition, the ratio of GABAergic inputs is higher on calbindin- than on parvalbumin-containing neurons (Gulyas et al., 1999). These findings suggest that the parvalbumin-containing neurons, which receive more excitatory inputs but fewer inhibitory inputs than do calbindin neurons, could be more sensitive to excitotoxic effects. Unfortunately, similar data are not available for somatostatin-containing interneurons to date. Nevertheless, it is likely that additional factors are involved in determining the sensitivity of specific groups of neurons to damage since, as discussed previously, many parvalbumin-containing neurons are also resistant to excitotoxicity.

Since the loss of GABAergic interneurons is restricted to the stratum oriens, the afferent inputs from collaterals of CA1 pyramidal cells to some of these interneurons could be an additional factor contributing to their vulnerability. Indeed, previous morphological and electrophysiological studies demonstrated that stratum oriens/alveus interneurons, including somatostatin-containing O-LM cells and some perisomatic interneurons, are innervated by axon collaterals of local CA1 pyramidal cells (Lacaille et al., 1987; Blasco-Ibanez and Freund, 1995; Maccaferri and McBain, 1995, 1996), and many of these neurons degenerate after excitotoxic damage. However, calbindin-containing interneurons at the stratum oriens/alveus border receive similar afferents (Blasco-Ibanez and Freund, 1995) but are resistant in this model, further suggesting that the vulnerability of specific groups of stratum oriens interneurons is certainly multifactorial.

Vulnerability of other stratum oriens neurons

While the loss of GABAergic neurons is extensive, our data suggest that some non-GABAergic neurons also degenerate. A loss of neurons only labeled for NeuN is also observed in the stratum oriens of CA1 in pilocarpine-treated animals. These neurons, located close to the pyramidal cell layer, could be ectopic pyramidal cells. As is the case for some stratum oriens interneurons, the vulnerability of these ectopic CA1 pyramidal neurons could be related to the number of excitatory inputs received by these cells. Indeed, morphological studies demonstrated that pyramidal cells with somata further away from the stratum pyramidale/stratum radiatum border had greater dendritic length in the stratum oriens than did pyramidal cells with their somata close to this border (Bannister and Larkman, 1995). Since the relative proportion of dendritic length in the different layers should determine the spectrum of synaptic input on these cells, and the pyramidal cells receive axon collaterals from other pyramidal cells (Thomson and Radpour, 1991; Deuchars and Thomson, 1996) and giant cells (Gulyas et al., 1998), ectopic pyramidal cells are likely to be more influenced by these local glutamatergic afferents and thus could be more vulnerable.

Functional consequences

The integrative properties and activity of neurons depend strongly on the ratio and spatial distribution of excitatory and inhibitory synaptic inputs they receive. On CA1 pyramidal cells, inhibitory inputs are mainly concentrated in the perisomatic region and on the dendrites in stratum lacunosum-moleculare (Megias et al., 2001). Therefore, a substantial loss of stratum oriens interneurons, including somatostatin-containing O-LM cells that participate in dendritic inhibition and parvalbumin-containing axo-axonic cells that control action potential generation of principal cells (Miles et al., 1996), would be expected to result in strong deficits of inhibition and imbalance in favor of excitation. Indeed, electrophysiological data (Cossart et al., 2001) have clearly demonstrated, in this model of TLE, a marked reduction of GABAergic inhibition in the dendrites of pyramidal cells, a reduction which is well correlated with the loss of somatostatin-containing O-LM cells.

In contrast, our results regarding the loss of parvalbumin-containing axo-axonic cells seem at odds with data obtained from electrophysiological studies performed in the same model. These studies reported that perisomatic inhibition is still functional (Esclapez et al., 1997) and is even increased (Hirsch et al., 1999; Cossart at al., 2001) in the somata of CA1 pyramidal cells in pilocarpine-treated animals with spontaneous recurrent seizures. One hypothesis to explain such a discrepancy is that the activity of the resistant basket cells could mask a deficit of inhibition occurring on the AIS of CA1 pyramidal neurons, where axo-axonic cells terminate. Indeed, several lines of evidence converge to demonstrate a hyperactivity of remaining GABAergic neurons including basket cells in these epileptic animals (Esclapez et al., 1997; Esclapez and Houser, 1999; Cossart et al., 2001). In addition, other mechanisms could contribute to the compensation for the loss of inhibitory synapses on the AISs, for example, an upregulation of GABA-A receptors, although this has yet to be demonstrated in the AIS.

Despite an enhancement of the activity-dependent inhibition on the soma of CA1 pyramidal cells, a decrease of miniature IPSC (action potential-independent inhibitory postsynaptic current) frequency is observed in pilocarpine-treated animals (Hirsch et al., 1999). The reason for this decrease is still unknown. Our results raise the possibility that the component of perisomatic inhibition supplied by miniature events may derive

largely from axo-axonic cells and therefore the loss of these interneurons and of their synapses from the AIS of pyramidal cells could lead to a decrease of GABAergic miniature events described in these animals.

Regardless of the lack of direct physiological evidence confirming a loss of inhibition on the AIS of CA1 pyramidal cells, our data strongly suggest that mechanisms controlling the generation of action potentials in CA1 pyramidal neurons are also impaired in this model of TLE. This alteration could participate in the generation of the paroxysmal burst activity recorded in the CA1 pyramidal neurons of these epileptic animals (Esclapez et al., 1997,1999; Cossart et al., 2001).

CONCLUSION

The present findings demonstrate that two main subpopulations of neurochemically identified interneurons are responsible for the loss of GABAergic neurons in the stratum oriens of CA1 in pilocarpine-treated animals; i.e., the somatostatin- and parvalbumin-containing neurons. Among these neurons, our results emphasize the vulnerability of two specific types: the somatostatin-containing O-LM cells responsible for dendritic inhibition and the parvalbumin-containing axo-axonic cells exerting perisomatic inhibition. Thus, two specific groups of interneurons controlling the major input and output sites of CA1 pyramidal cells are impaired in this model of TLE. The causal relationship between recurrent seizure activity and impairment of either or both of these inhibitory functions remains to be established.

ACKNOWLEDGMENTS

We thank Dr. Z.S. Magloczky and L. Wittner for helpful assistance with electron microscopy and Lynda El Hassar, Sylvain Rama, and Nadine Ferrand for excellent assistance with immunohistological and histological experiments.

LITERATURE CITED

Andre V, Marescaux C, Nehlig A, Fritschy JM. 2001. Alterations of hippocampal GABAergic system contribute to development of spontaneous recurrent seizures in the rat lithium-pilocarpine model of temporal lobe epilepsy. Hippocampus 11:452–468.

Bannister NJ, Larkman AU. 1995. Dendritic morphology of CA1 pyramidal neurones from the rat hippocampus. I. Branching patterns. J Comp Neurol 360:150–160.

Benoit R, Bohlen P, Ling N, Esch F, Baird A, Ying SY, Wehrenberg WB, Guillemin R, Morrison JH, Bakhit C. 1985. Somatostatin-28 [1-12]-like peptides. Adv Exp Med Biol 188:89–107.

Bering R, Diemer NH, Draguhn A, Johansen FF. 1995. Co-localization of somatostatin mRNA and parvalbumin in the dorsal rat hippocampus after cerebral ischemia. Hippocampus 5:341–348.

Best N, Mitchell J, Baimbridge KG, Wheal HV. 1993. Changes in parvalbumin-immunoreactive neurons in the rat hippocampus following a kainic acid lesion. Neurosci Lett 28;155:1–6.

Best N, Mitchell J, Wheal HV. 1994. Ultrastructure of parvalbumin-immunoreactive neurons in the CA1 area of the rat hippocampus following a kainic acid injection. Acta Neuropathol (Berl) 87:187–195.

Blasco-Ibanez JM, Freund TF. 1995. Synaptic input of horizontal interneurons in stratum oriens of the hippocampal CA1 subfield: structural basis of feedback activation. Eur J Neurosci 7:2170–2180.

Bouilleret V, Loup F, Kiener T, Marescaux C, Fritschy JM. 2000. Early loss of interneurons and delayed subunit-specific changes in GABA(A)-receptor expression in a mouse model of mesial temporal lobe epilepsy. Hippocampus 10:305–324.

Buckmaster PS, Dudek FE. 1997. Neuron loss, granule cell axon reorganization, and functional changes in the dentate gyrus of epileptic kainate-treated rats. J Comp Neurol 385:385–404.

Buckmaster PS, Jongen-Relo AL. 1999. Highly specific neuron loss preserves lateral inhibitory circuits in the dentate gyrus of kainate-induced epileptic rats. J Neurosci 19:9519–9529.

Cavalheiro EA, Silva DF, Turski WA, Calderazzo-Filho LS, Bortolotto ZA, Turski L. 1987. The susceptibility of rats to pilocarpine-induced seizures is age-dependent. Dev Brain Res 37:43–58.

Celio MR, Baier W, Scharer L, de Viragh PA, Gerday C. 1988. Monoclonal antibodies directed against the calcium binding protein parvalbumin. Cell Calcium 9:81–86.

Celio MR, Baier W, Scharer L, Gregersen HJ, de Viragh PA, Norman AW. 1990. Monoclonal antibodies directed against the calcium binding protein Calbindin D-28k. Cell Calcium 11:599–602.

Cossart R, Dinocourt C, Hirsch JC, Merchan-Perez A, De Felipe J, Ben-Ari Y, Esclapez M, Bernard C. 2001. Dendritic but not somatic GABAergic inhibition is decreased in experimental epilepsy. Nat Neurosci 4:52–62.

de Lanerolle NC, Kim JH, Robbins RJ, Spencer DD. 1989. Hippocampal interneuron loss and plasticity in human temporal lobe epilepsy. Brain Res 495:387–395.

DeFelipe J. 1999. Chandelier cells and epilepsy. Brain 122:1807–1822.

Deuchars J, Thomson AM. 1996. CA1 pyramid-pyramid connections in rat hippocampus in vitro: dual intracellular recordings with biocytin filling. Neuroscience 74:1009–1018.

Dinocourt C, Ben-Ari Y, Esclapez M. 2001. Loss of somatostatin and/or parvalbumin containing neurons in the stratum oriens of CA1 in experimental temporal lobe epilepsy. Soc Neurosci Abstr 557.8.

Erlander MG, Tillakaratne NJ, Feldblum S, Patel N, Tobin AJ. 1991. Two genes encode distinct glutamate decarboxylases. Neuron 7:91–100.

Esclapez M, Houser CR. 1999. Up-regulation of GAD65 and GAD67 in remaining hippocampal GABA neurons in a model of temporal lobe epilepsy. J Comp Neurol 412:488–505.

Esclapez M, Tillakaratne NJ, Tobin AJ, Houser CR. 1993. Comparative localization of mRNAs encoding two forms of glutamic acid decarboxylase with nonradioactive in situ hybridization methods. J Comp Neurol 331:339–362.

Esclapez M, Tillakaratne NJ, Kaufman DL, Tobin AJ, Houser CR. 1994. Comparative localization of two forms of glutamic acid decarboxylase and their mRNAs in rat brain supports the concept of functional differences between the forms. J Neurosci 14:1834–1855.

Esclapez M, Hirsch JC, Khazipov R, Ben-Ari Y, Bernard C. 1997. Operative GABAergic inhibition in hippocampal CA1 pyramidal neurons in experimental epilepsy. Proc Natl Acad Sci USA 94:12151–12156.

Esclapez M, Hirsch JC, Ben-Ari Y, Bernard C. 1999. Newly formed excitatory pathways provide a substrate for hyperexcitability in experimental temporal lobe epilepsy. J Comp Neurol 408:449–460.

Freund TF, Buzsaki G. 1996. Interneurons of the hippocampus. Hippocampus 6:347–470.

Freund TF, Buzsáki G, Leon A, Baimbridge KG, Somogyi P. 1990. Relationship of neuronal vulnerability and calcium binding protein immunoreactivity in ischemia. Exp Brain Res 83:55–66.

Freund TF, Ylinen A, Miettinen R, Pitkanen A, Lahtinen H, Baimbridge KG, Riekkinen PJ. 1991. Pattern of neuronal death in the rat hippocampus after status epilepticus. Relationship to calcium binding protein content and ischemic vulnerability. Brain Res Bull 28:27–38.

Gallyas F, Wolff JR, Bottcher H, Zaborszky L. 1980. A reliable and sensitive method to localize terminal degeneration and lysosomes in the central nervous system. Stain Technol 55:299–306.

Gorter JA, van Vliet EA, Aronica E, Lopes da Silva FH. 2001. Progression of spontaneous seizures after status epilepticus is associated with mossy fibre sprouting and extensive bilateral loss of hilar parvalbumin and somatostatin-immunoreactive neurons. Eur J Neurosci 13:657–669.

Gulyas AI, Hajos N, Freund TF. 1996. Interneurons containing calretinin are specialized to control other interneurons in the rat hippocampus. J Neurosci 16:3397–3411.

Gulyas AI, Toth K, McBain CJ, Freund TF. 1998. Stratum radiatum giant cells: a type of principal cell in the rat hippocampus. Eur J Neurosci 10:3813–3822.

Gulyas AI, Megias M, Emri Z, Freund TF. 1999. Total number and ratio of excitatory and inhibitory synapses converging onto single interneurons of different types in the CA1 area of the rat hippocampus. J Neurosci 19:10082–10097.

Gulyas AI, Hajos N, Sik A, Freund TF. 2001. Septally Projecting nonprincipal cells of the rat hippocampus posses local axon collaterals and

are modulated by transmitters of subcortical pathways. Soc Neurosci Abstr 847.4.

Hirsch JC, Agassandian C, Merchan-Perez A, Ben-Ari Y, DeFelipe J, Esclapez M, Bernard C. 1999. Deficit of quantal release of GABA in experimental models of temporal lobe epilepsy. Nat Neurosci 2:499–500.

Houser CR, Esclapez M. 1994. Localization of mRNAs encoding two forms of glutamic acid decarboxylase in the rat hippocampal formation. Hippocampus 4:530–545.

Houser CR, Esclapez M. 1996. Vulnerability and plasticity of the GABA system in the pilocarpine model of spontaneous recurrent seizures. Epilepsy Res 26:207–218.

Jinno S, Kosaka T. 2000. Colocalization of parvalbumin and somatostatin-like immunoreactivity in the mouse hippocampus: quantitative analysis with optical dissector. J Comp Neurol 428:377–388.

Katona I, Acsady L, Freund TF. 1999. Postsynaptic targets of somatostatin-immunoreactive interneurons in the rat hippocampus. Neuroscience 88:37–55.

Katsumaru H, Kosaka T, Heizmann CW, Hama K. 1988. Immunocytochemical study of GABAergic neurons containing the calcium-binding protein parvalbumin in the rat hippocampus. Exp Brain Res 72:347–362.

Kaufman DL, Houser CR, Tobin AJ. 1991. Two forms of the gamma-aminobutyric acid synthetic enzyme glutamate decarboxylase have distinct intraneuronal distributions and cofactor interactions. J Neurochem 56:720–723.

Kobayashi Y, Kaufman DL., Tobin AJ. 1987. Glutamic acid decarboxylase cDNA: nucleotide sequence encoding an enzymatically active fusion protein. J Neurosci 7:2768–2772.

Kosaka T, Katsumaru H, Hama K, Wu JY, Heizmann CW. 1987. GABAergic neurons containing the Ca2+-binding protein parvalbumin in the rat hippocampus and dentate gyrus. Brain Res 419:119–130.

Kosaka T, Wu JY, Benoit R. 1988. GABAergic neurons containing somatostatin-like immunoreactivity in the rat hippocampus and dentate gyrus. Exp Brain Res 71:388–398.

Lacaille JC, Mueller AL, Kunkel DD, Schwartzkroin PA. 1987. Local circuit interactions between oriens/alveus interneurons and CA1 pyramidal cells in hippocampal slices: electrophysiology and morphology. J Neurosci 7:1979–1993.

Li XG, Somogyi P, Tepper JM, Buzsaki G. 1992. Axonal and dendritic arborization of an intracellularly labeled chandelier cell in the CA1 region of the rat hippocampus. Exp Brain Res 90:519–525.

Lu W, Haber SN. 1992. In situ hybridization histochemistry: a new method for processing material stored for several years. Brain Res 578:155–160.

Maccaferri G, McBain CJ. 1995. Passive propagation of LTD to stratum oriens-alveus inhibitory neurons modulates the temporoammonic input to the hippocampal CA1 region. Neuron 15:137–145.

Maccaferri G, McBain CJ. 1996. Long-term potentiation in distinct subtypes of hippocampal nonpyramidal neurons. J Neurosci 16:5334–5343.

Maccaferri G, Roberts JD, Szucs P, Cottingham CA, Somogyi P. 2000. Cell surface domain specific postsynaptic currents evoked by identified GABAergic neurones in rat hippocampus in vitro. J Physiol 524:91–116.

Magloczky Z, Freund TF. 1995. Delayed cell death in the contralateral hippocampus following kainate injections into the CA3 subfield. Neuroscience 66:847–860.

Magloczky Z, Wittner L, Borhegyi Z, Halasz P, Vajda J, Czirjak S, Freund TF. 2000. Changes in the distribution and connectivity of interneurons in the epileptic human dentate gyrus. Neuroscience 96:7–25.

Marco P, Sola RG, Pulido P, Alijarde MT, Sanchez A, Ramon y Cajal S, DeFelipe J. 1996. Inhibitory neurons in the human epileptogenic temporal neocortex. An immunocytochemical study. Brain 119:1327–1347

Marco P, Sola RG, Ramon y Cajal S, DeFelipe J. 1997. Loss of inhibitory synapses on the soma and axon initial segment of pyramidal cells in human epileptic peritumoural neocortex: implications for epilepsy. Brain Res Bull 44:47–66.

Mathern GW, Babb TL, Pretorius JK, Leite JP. 1995 Reactive synaptogenesis and neuron densities for neuropeptide Y, somatostatin, and glutamate decarboxylase immunoreactivity in the epileptogenic human fascia dentata. J Neurosci 15:3990–4004.

McBain CJ, Fisahn A. 2001. Interneurons unbound. Nat Rev Neurosci 2:11–23.

Megias M, Emri Z, Freund TF, Gulyas AI. 2001. Total number and distribution of inhibitory and excitatory synapses on hippocampal CA1 pyramidal cells. Neuroscience 102:527–540.

Miles R, Toth K, Gulyas AI, Hajos N, Freund TF. 1996. Differences between somatic and dendritic inhibition in the hippocampus. Neuron 16:815–823.

Morin F, Beaulieu C, Lacaille JC. 1998. Selective loss of GABA neurons in area CA1 of the rat hippocampus after intraventricular kainate. Epilepsy Res 32:363–369.

Mullen RJ, Buck CR, Smith AM. 1992. NeuN, a neuronal specific nuclear protein in vertebrates. Development 116:201–211.

Nadler JV, Evenson DA. 1983. Use of excitatory amino acids to make axon-sparing lesions of hypothalamus. Methods Enzymol 103:393–400.

Obenaus A, Esclapez M, Houser CR. 1993. Loss of glutamate decarboxylase mRNA-containing neurons in the rat dentate gyrus following pilocarpine-induced seizures. J Neurosci 13:4470–4485.

Pawelzik H, Hughes DI, Thomson AM. 2002. Physiological and morphological diversity of immunocytochemically defined parvalbumin- and cholecystokinin-positive interneurones in CA1 of the adult rat hippocampus. J Comp Neurol 443:346–367.

Peters A, Palay SL, Webster HdeF. 1991. The fine structure of the nervous system. New York: Oxford University Press.

Racine RJ. 1972. Modification of seizure activity by electrical stimulation. II. Motor seizure. Electroencephalogr Clin Neurophysiol 32:281–294.

Rempe DA, Bertram EH, Williamson JM, Lothman EW. 1997. Interneurons in area CA1 stratum radiatum and stratum oriens remain functionally connected to excitatory synaptic input in chronically epileptic animals. J Neurophysiol 78:1504–1515.

Richoux JP, Seyer R, Castro B, Rivaille P, Dubois MP, Grignon G. 1981. Preparation of antisera against some sequences of somatostatin synthesized on resin. Application to the immunological detection of somatostatin systems: preliminary results. J Physiol 77:985–988.

Robbins RJ, Brines ML, Kim JH, Adrian T, de Lanerolle N, Welsh S, Spencer DD. 1991. A selective loss of somatostatin in the hippocampus of patients with temporal lobe epilepsy. Ann Neurol 29:325–332.

Schmued LC, Hopkins KJ. 2000. Fluoro-Jade B: a high affinity fluorescent marker for the localization of neuronal degeneration. Brain Res 874: 123–130.

Sik A, Penttonen M, Ylinen A, Buzsaki G. 1995. Hippocampal CA1 interneurons: an in vivo intracellular labeling study. J Neurosci 15:6651–6665.

Sloviter RS. 1987. Decreased hippocampal inhibition and a selective loss of interneurons in experimental epilepsy. Science 235:73–76.

Sloviter RS. 1991. Permanently altered hippocampal structure, excitability, and inhibition after experimental status epilepticus in the rat: the "dormant basket cell" hypothesis and its possible relevance to temporal lobe epilepsy. Hippocampus 1:41–66.

Somogyi P, Hodgson AJ, Smith AD, Nunzi MG, Gorio A, Wu JY. 1984. Different populations of GABAergic neurons in the visual cortex and hippocampus of cat contain somatostatin- or cholecystokinin-immunoreactive material. J Neurosci 4:2590–2603.

Sperk G, Marksteiner J, Gruber B, Bellmann R, Mahata M, Ortler M. 1992. Functional changes in neuropeptide Y- and somatostatin-containing neurons induced by limbic seizures in the rat. Neuroscience 50:831–846

Thomson AM, Radpour S. 1991. Excitatory connections between CA1 pyramidal cells revealed by spike triggered averaging in slices of rat hippocampus are partially NMDA receptor mediated. Eur J Neurosci 3:587–601.

Toth K, Freund TF. 1992. Calbindin D28k-containing nonpyramidal cells in the rat hippocampus: their immunoreactivity for GABA and projection to the medial septum. Neuroscience 49:793–805.

Turski WA, Cavalheiro EA, Schwarz M, Czuczwar SJ, Kleinrok Z, Turski L. 1983. Limbic seizures produced by pilocarpine in rats: behavioural, electroencephalographic and neuropathological study. Behav Brain Res 9:315–335.

Watson RE Jr, Wiegand SJ, Clough RW, Hoffman GE. 1986. Use of cryoprotectant to maintain long-term peptide immunoreactivity and tissue morphology. Peptides 7:155–159.

West MJ. 1999. Stereological methods for estimating the total number of neurons and synapses: issues of precision and bias. Trends Neurosci 22:51–61.

West MJ, Slomianka L, Gundersen HJ. 1991. Unbiased stereological estimation of the total number of neurons in the subdivisions of the rat hippocampus using the optical fractionator. Anat Rec 231:482–497.

Wittner L, Magloczky Z, Borhegyi Z, Halasz P, Toth S, Eross L, Szabo Z, Freund TF. 2001. Preservation of perisomatic inhibitory input of granule cells in the epileptic human dentate gyrus. Neuroscience 108:587–600.

Ylinen AMA, Miettinen R, Pitkanen A, Gulyas AI, Freund TF, Riekkinen PJ. 1991. Enhanced GABAergic inhibition preserves hippocampal structure and function in a model of epilepsy. Proc Natl Acad Sci USA 88:7650–7653.